CHARACTERISTICS OF THE TORNADO ENVIRONMENT AS DEDUCED FROM PROXIMITY SOUNDINGS

by

Thomas G. Wills

Preparation of this report
has been supported by
NSF GF - 287
ESSA E - 22 - 80 - 68(G)

Department of Atmospheric Science
Colorado State University
Fort Collins, Colorado

June, 1969

Atmospheric Science Paper No. 140

TABLE OF CONTENTS

ABSTRACT

An observational study of 700 tornado proximity soundings is presented. Soundings were chosen that were within two hours and 100 miles from well-documented tornadoes. Data was obtained during the period of 1956-1966 and covers all areas of the U.S. east of the Rocky Mountains. Tropical storm-spawned tornado soundings are also included. Soundings were sorted by geographical region, time, and position relative to the tornado location.

A summary of the characteristics of the proximity soundings is described with regard to the tornado's environmental horizontal wind fields, vertical wind shear, and cumulus potential buoyancy. The magnitude of the lower tropospheric (below 500 mb) vertical wind shear was found to be very large--averaging 44 knots. The horizontal wind fields demonstrate a variable shear across the tornado and an apparent "blocking" of the mean wind field at upper levels created by large cumulonimbus clouds penetrating through the vertically shearing environment. When the lapse-rate and surface convergence dictate that cumulonimbus convection is likely, then the most crucial parameter for tornado occurrence is the vertical wind shear in the lower half of the troposphere.

A "tornado-likelihood" index is developed utilizing the three parameters of cumulus potential buoyancy, low-level convergence, and lower tropospheric vertical wind shear. When tested in comparison with non-tornadic days, this index appears to be a good predictor.

I. INTRODUCTION

The study of the tornado environment through the use of proximity soundings is not new. Many investigators such as Fawbush and Miller (1952, 1954), Beebe (1958), Miller (1967a), and Darkow (1967, 1969), have presented mean thermodynamic characteristics for various tornadic air masses. In addition, several indices relating temperature and moisture characteristics to the potential instability have been developed and discussed by Showalter (1953), Galway (1956), Miller, Waters and Bartlett (1967), and Darkow (op. cit.).

The above studies of the tornado environment, however, have primarily utilized only thermodynamic criteria. The vertical wind shear characteristics and the synoptic scale horizontal flow patterns in the tornado environment have not yet been numerically categorized for large data samples. Also, wind observations have not yet been directly incorporated into a tornado forecast index. This study presents information on the combined vertical and horizontal distribution of the horizontal winds and on the thermodynamic characteristics associated with various tornado environments in the U.S. A severe weather forecasting index which incorporates a thermodynamic parameter and a vertical wind shear parameter is developed.

Endlich and Mancuso's (1967) computer adaptation of Crumrine's (1965) mention of the 850 mb to 500 mb vertical wind shear as a useful forecasting tool is the only explicit mention to date of the

vertical wind shear in a forecasting index. The physical reasoning for the importance of this shear was related mainly to the generation of low-level cyclonic vorticity by the thermal wind. Little direct consideration has been given to vertical shear as a crucially important tornado forecasting parameter even though several theories [Newton and Newton (1959), Newton (1962), Bates (1967), Markgraf (1961), Wegener (1928), Bilancini (1962), and Gray (1969)] have emphasized that strong vertical wind shears are essential to the production of severe thunderstorms and their associated hail and tornadoes.

The role of vertical wind shear in the genesis of severe convective storms appears not to have been fully utilized for forecasting purposes. Miller (1967b), in an evaluation of the relative importance of 14 forecast parameters which favor the production of severe weather, does not directly mention vertical wind shear. He does, however, emphasize the importance of the low and middle level jets, which in an indirect sense, relate to the vertical shear.

If the tornado environment does have a characteristic shearing component, then a vertical wind shear parameter should be developed and incorporated into a tornado forecast index. The purpose of this investigation, then, has been to examine large numbers of tornado proximity soundings in an attempt to determine the characteristics and variability of the vertical and horizontal structure of the wind fields associated with the tornadic air mass and to look for evidences of additional forecast parameters.

Data Sources

The tornado proximity soundings used in this study cover the eleven-year period from 1956 to 1966. Tornado soundings were taken from all regions of the U.S. east of the Rocky Mountains. Soundings qualified as proximity soundings if:

1. There was a verified tornado occurrence within a 100 nautical-mile radius of the radiosonde station, and
2. The tornado occurrence was within two hours of sounding time.

Approximately 700 soundings met these requirements. These soundings were stratified by time of day, date, geographical region (Fig. 1) and location relative to frontal systems and air masses.

Tornado data was obtained from three sources:

1. Climatological Data National Summary for the years 1956-58,
2. Storm Data for the years 1959-63, and
3. The severe weather records of the National Severe Storms Forecast Center, Kansas City, Missouri, for the years 1964-66.

The radiosonde data was compiled from the Northern Hemispheric Data Tabulations.

Proximity sounding data and other information concerning time and location of the tornado was listed on punch cards and computer analyses were made. Each sounding was analyzed at standard levels* for temperature, dew point, u- and v-components, and vector

*Surface, 850 mb, 700 mb, 500 mb, 300 mb, and 200 mb.

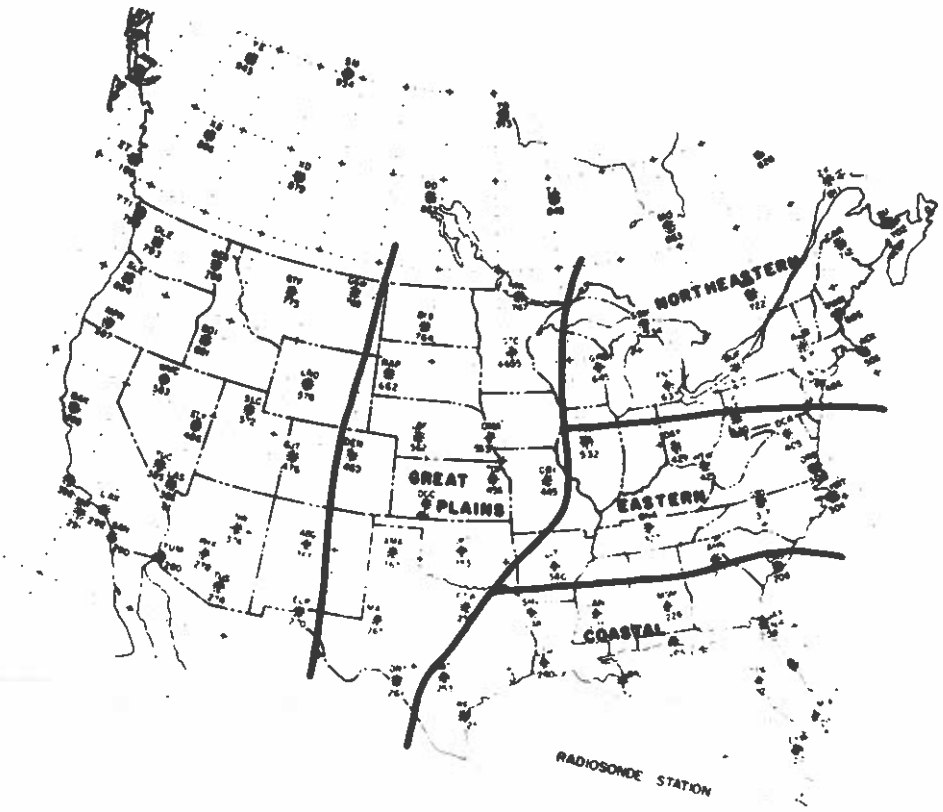

Fig. 1. Geographical regions into which the data has been divided.

wind. The u-shear, v-shear, and vector shears were calculated between all combinations of standard levels. In addition, computations of the means, standard deviations, and extremes of these parameters were made.

II. OBSERVED TORNADO ENVIRONMENT VERTICAL WIND SHEARS

The vertical wind shear is large for nearly all tornado soundings. Fig. 2 shows vertical vector shear profiles for the mean for all cases, the four geographical regions, and a special group of 30 tropical storm induced proximity soundings (all that are available from historical records). Note the large magnitude of the vector shears in the lower half of the troposphere in all profiles. The average shear between the surface and 500 mb is 41 knots. While the Coastal profile exhibits slightly less shear, and the Northeastern region has slightly more shear, there appears to be no significant difference between the shear profiles based on geographical location. Fig. 3 shows the magnitude of shear per 100 mb between various standard pressure thicknesses and Fig. 4 presents the magnitude of shear per kilometer. A striking observation is evident from these figures--the majority of the shear noted in the tornado environment occurs in the lowest layers of the troposphere. One-half of the vertical shear which is present in the troposphere occurs below 700 mb (or 3 km).

Tropical Storm Cases

The mean shear profile for the tropical storm induced tornadoes is markedly different from the mid-latitude profiles. The layer of maximum shear is between the surface and 850 mb. Above

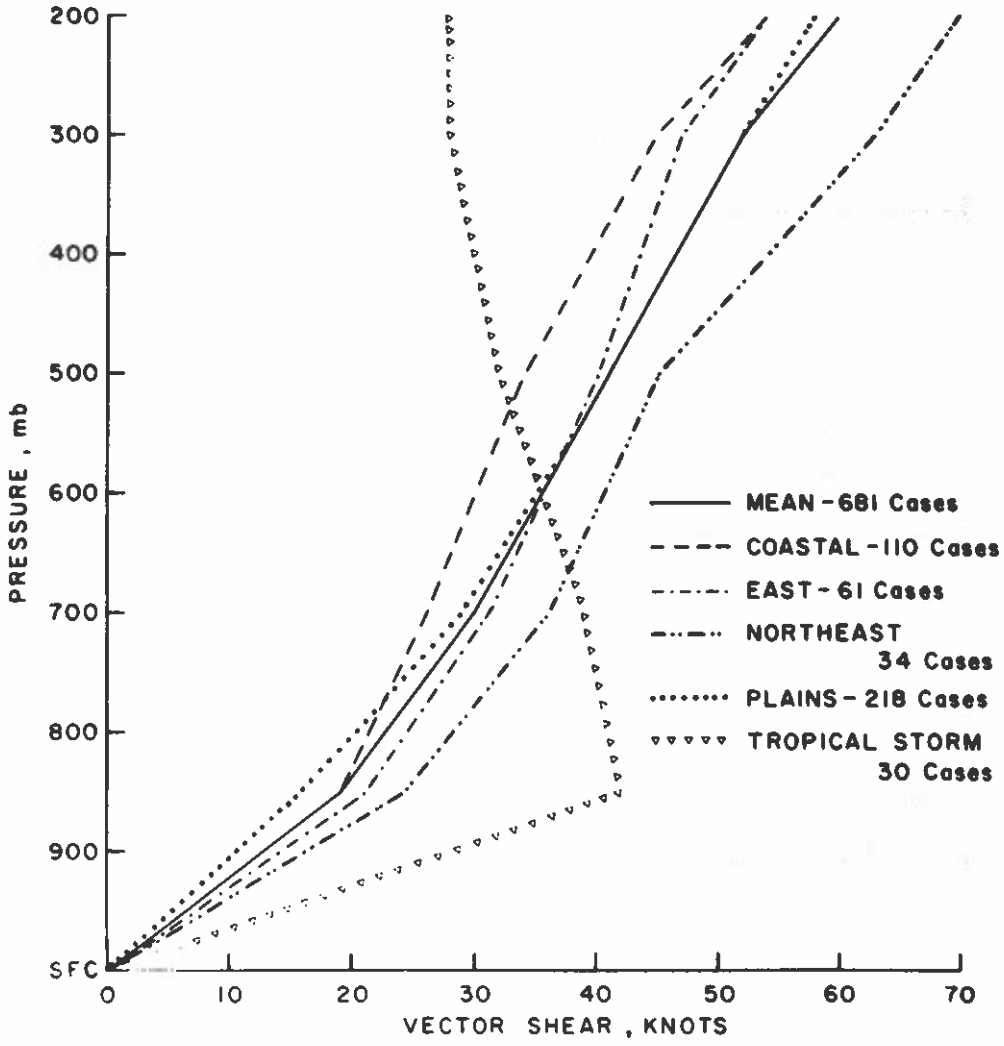

Fig. 2. Profiles of the average magnitude of the observed tornado environment vertical vector wind shear for four selected geographical regions, tropical storm induced cases, and all mid-latitude cases. The shear is computed at standard pressure levels with respect to the surface wind.

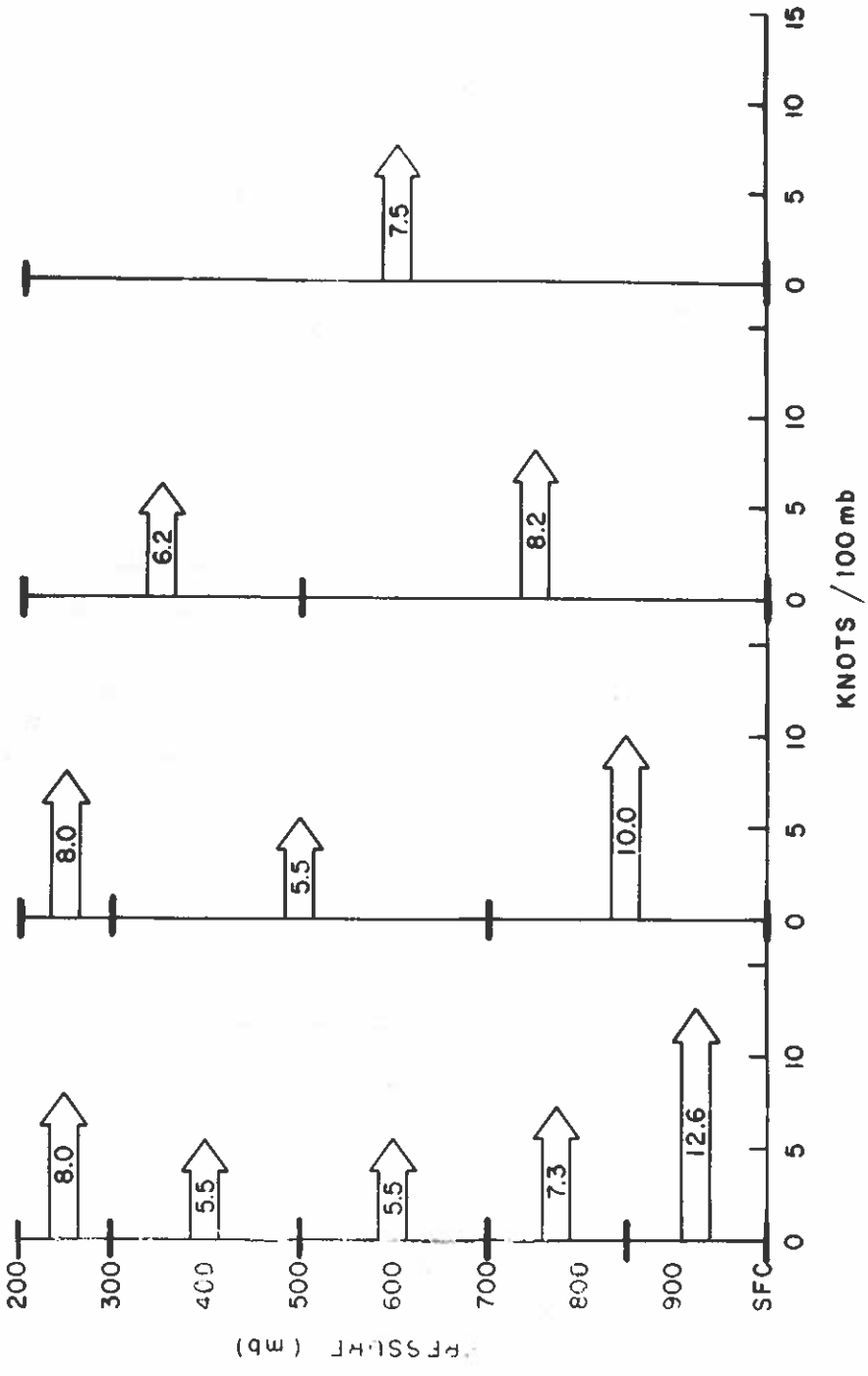

Fig. 3. Average magnitude of the vertical vector wind shear between standard pressure surfaces for the mid-latitude tornado environment. Selected standard pressure surfaces are marked with tick-marks along the vertical axes. The average shear (in knots per 100 mb) between any two consecutive tick-marks (pressure levels) is given by the horizontal arrow centered between the two tick-marks.

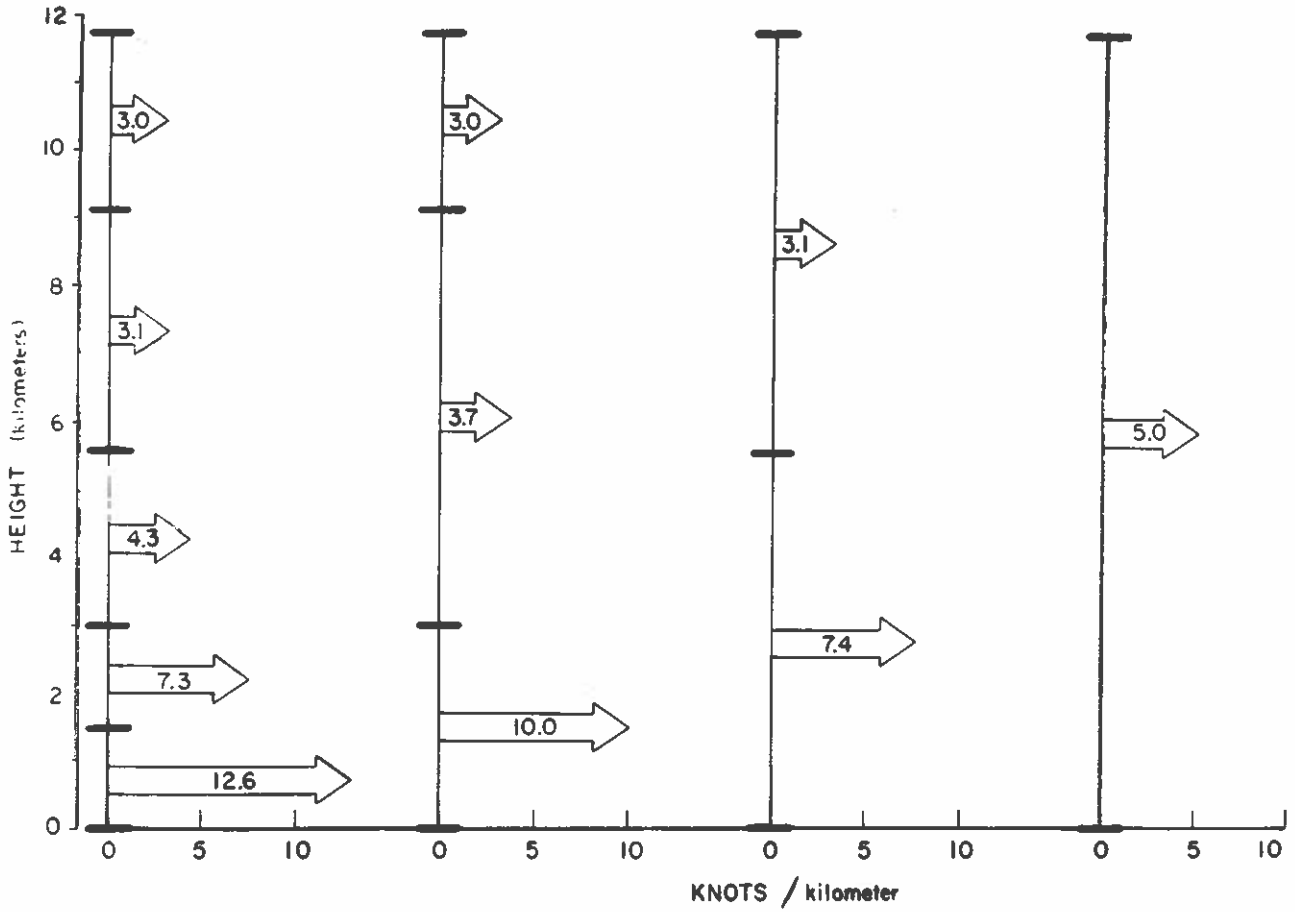

Fig. 4. Average magnitude of the vertical vector wind shear between standrad pressure surfaces for the mid-latitude tornado environment. The vertical axes are linear with height. Selected standard pressure surfaces are marked with tick-marks along the vertical axes. The average shear (in knots per km) between any two consecutive tick-marks (pressure levels) is given by the horizontal arrow centered between the two tick-marks.

this layer of maximum shear, the wind speeds (and the resulting vector shears) decrease with height. This is in direct contrast to the mid-latitude profiles which show steadily increasing shear with height. Fig. 5 shows the average magnitude of vertical shear per kilometer for the tropical storm cases. Here the positive vertical shear is concentrated in a very small layer (surface to 850 mb). The shear is then negative throughout the rest of the troposphere.

The most surprising characteristic of these tropical storm induced tornado soundings is the relatively low surface wind speeds which average only 18 knots. The 850 mb wind velocities, on the other hand, average no less than 55 knots. This was not to have been expected in the tropical storm where winds typically decrease with height.

This observed strong positive vertical shear, resulting from the apparent breakdown of the surface winds as the tropical storm moves over land, is not without explanation. As the tropical storm moves over land the oceanic heat and moisture source is removed. The inward spiraling air in the boundary layer of that part of the storm over land is being cooled by expansion. The radial temperature gradient in the lowest layer is reversed. This causes a rapid breakdown of the surface winds and the observed strong positive vertical wind shear from the surface to 850 mb. Thus, the tropical storm begins to dissipate in the surface layers first while simultaneously creating a low-level positive vertical shearing environment similar

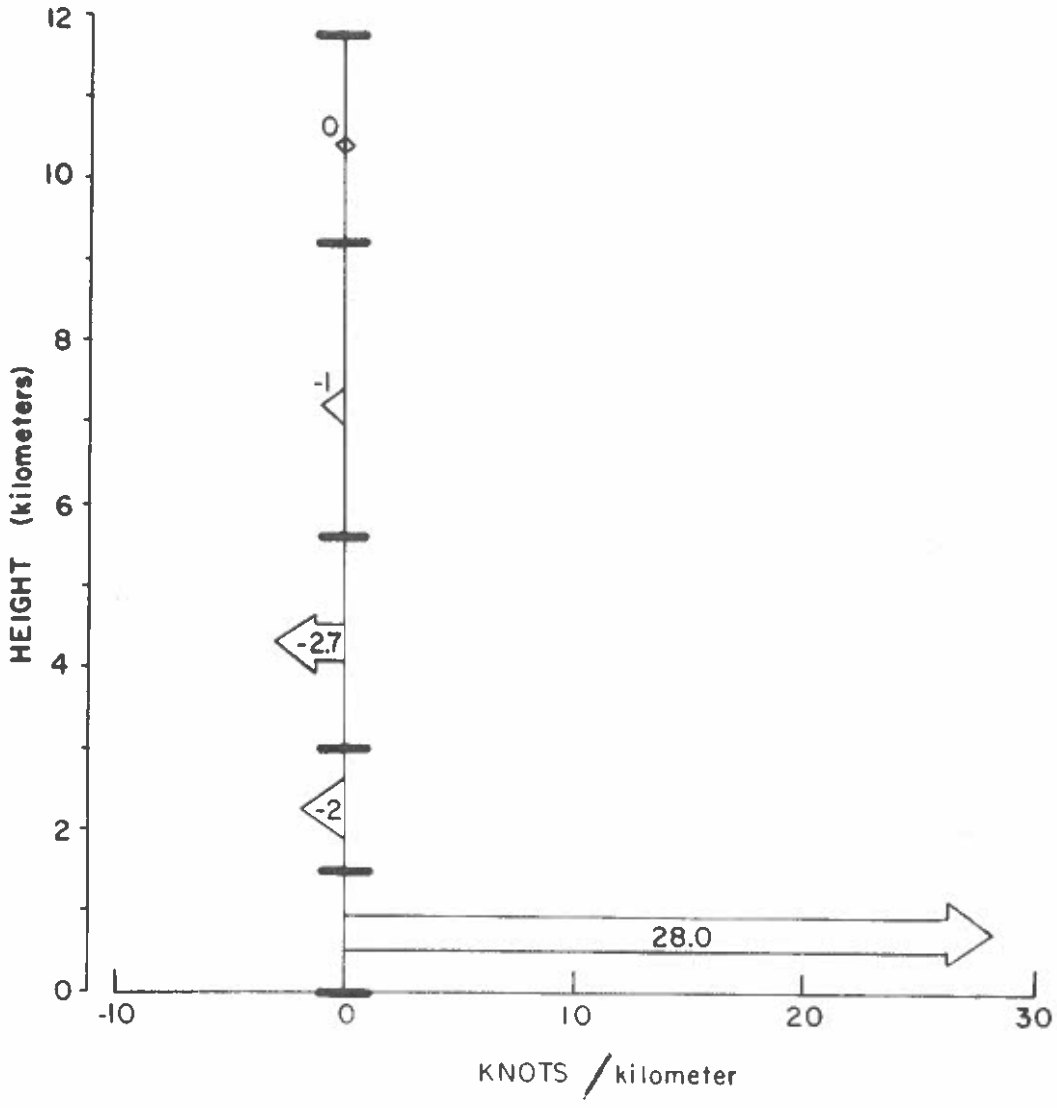

Fig. 5. Average magnitude of the vertical vector wind shear between standard pressure surfaces for the tropical storm spawned tornado environment. The vertical axes are linear withheight. Selected standard pressure surfaces are marked with tick-marks along the vertical axes. The average shear (in knots per km) between any two consecutive tick-marks (pressure levels) is given by the horizontal arrow centered between the two tick-marks.

to that in mid-latitude tornado cases.

Magnitude of Strongest Lower Layer Shear

The individual lower tropospheric shear profiles are not nearly as smooth as the mean profiles of Fig. 2 suggest. The surface to 500 mb shear is not always the best representation of the largest lower level shear. In order to obtain the best representation of the mean maximum lower tropospheric shear available in the tornado environment, the strongest shear between any two standard levels below 500 mb (i.e., surface to 700 mb, 850 mb to 500 mb, etc.) was determined for each sounding. The magnitudes of these strongest lower tropospheric shears were then averaged to determine a mean strongest lower layer shear, which is portrayed in Fig. 6. Again, no significant differences are noted between the geographical regions. The mean of all cases is 44 knots. The 49 knot mean shear for the tropical storm cases is the largest of the mean layer shears.

Since the wind data reported from rawinsondes is a smoothed, time-averaged value, the small time and distance scale variations of the wind are not detected. Thus, it is probable that the actual shearing conditions at individual tornado locations are considerably larger than the values reported here.

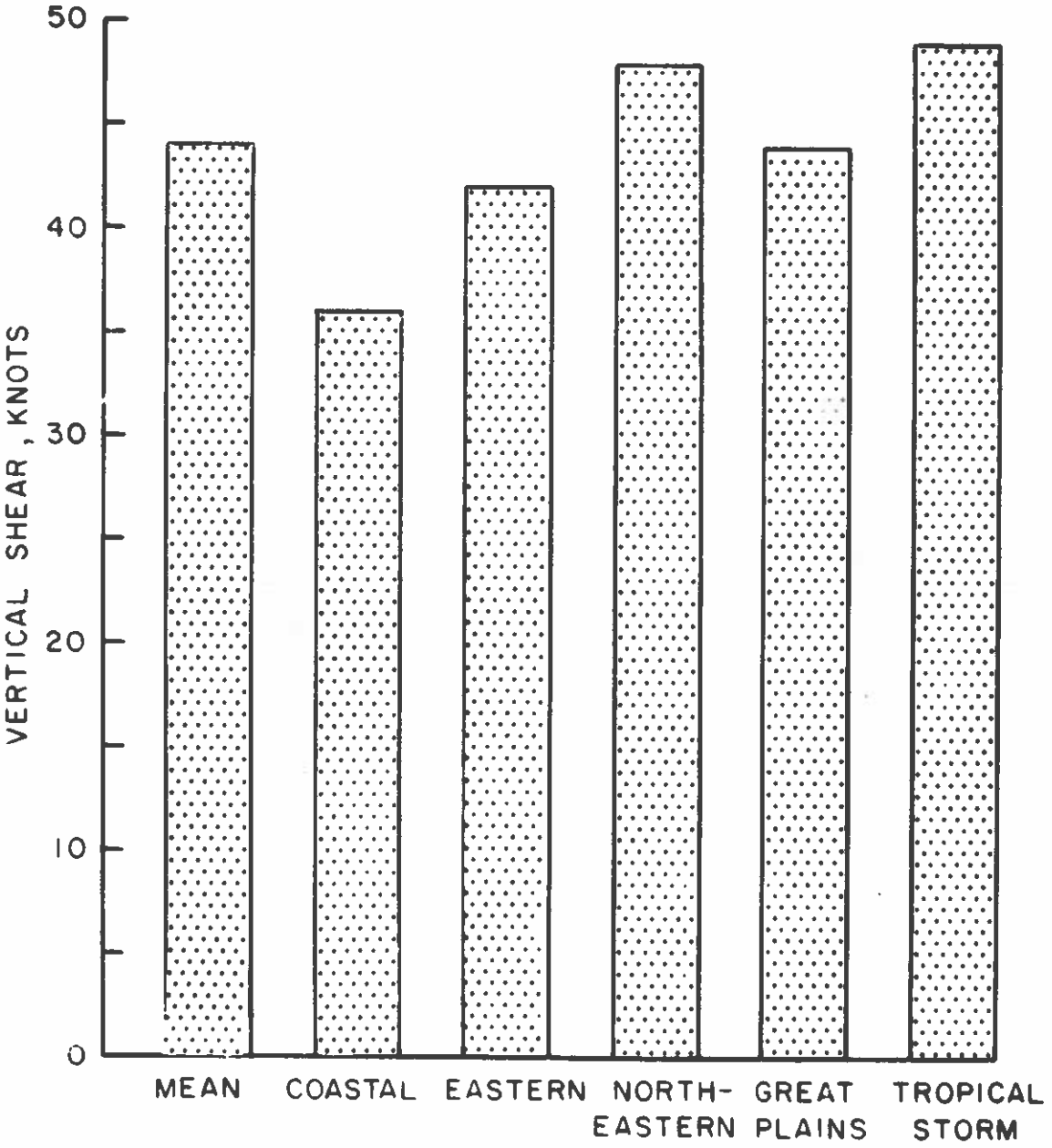

Fig. 6. Average magnitude of the strongest vertical vector wind shear within any lower tropospheric layer for four selected geographical regions, tropical storm induced cases, and all mid-latitude cases.

III. OBSERVED HORIZONTAL WIND FIELDS SURROUNDING 220 GREAT PLAINS TORNADOES

In order to obtain information on the horizontal wind field surrounding tornadoes, the wind fields of 220 Great Plains cases from the months of April, May, and June were composited in a coordinate system centered on the tornado's center. Data was categorized with respect to its distance and direction from the tornado. Soundings were broken into two radial groups--those within 50 miles of the tornado, and those between 50 and 100 miles from the tornado. Each sounding was then placed into one of eight 45° azimuthal groups (0 - 45 degrees, 46 - 90 degrees, etc.). All data within each of the 16 horizontal groupings was averaged and composited for each standard level. Maps of the tornado environmental wind fields were then plotted. Figs. 7, 10, 13, 16, 19, 22, and 25 show the mean wind fields at all standard levels. (100 mb data was used for this presentation to portray the winds above the normal cloud top height.)

Surface winds (Fig. 7) are from the south and southeast. Note that the wind speeds are strongest to the south and east of the center. This indicates a cyclonic relative vorticity over the region and the probability of an Ekman type frictionally forced convergence.

At 850 mb (Fig. 10), the winds are from the south to southwesterly direction. They are again strongest to the south and east of the tornado. The stronger winds to the east of the center are evidence of the low-level jet which has been cited as an important parameter in

forecasting severe weather (Miller, op. cit.). The position of the low-level jet agrees well with the statistics of Bonner (1963, 1965), and is in a position to give large cyclonic vorticity at the place of tornado occurrence. Low-level cyclonic vorticity is necessary for the production of frictionally induced cumulus clouds.

The winds veer and increase in magnitude from the surface to 700 mb and 500 mb (Figs. 13, 16). The mean 500 mb wind is 42 knots from a direction of 240 degrees. Winds at 300 mb and 200 mb (Figs. 19, 22) are also from 240 degrees. Wind velocity is a maximum at 200 mb. Wind speeds then begin to decrease and are much less at 100 mb (Fig. 25) but remain from the same direction.

A surprising feature of the upper level wind composites is the presence of weakening wind velocities (relative to the mean) on the immediate up- and downwind side from the tornado location. These weak wind regions coupled with the strong periferal winds to the NNW and SSE of the tornado show the probable "blocking" effect on the wind field created by cumulonimbus cloud clusters. This "blocking" of the mean wind field by large cumulonimbi was shown by Fujita and Arnold (1963) and Fujita and Grandoso (1968) from Doppler radar data taken during aircraft flights around a large isolated cumulonimbus cloud. The same effect has been shown by Fujita and Bradbury (1969) for an individual case based on satellite data. It was not expected that this likely blocking effect by large cumulonimbi clusters would show itself in a composite of a large data sample. The presence of such a

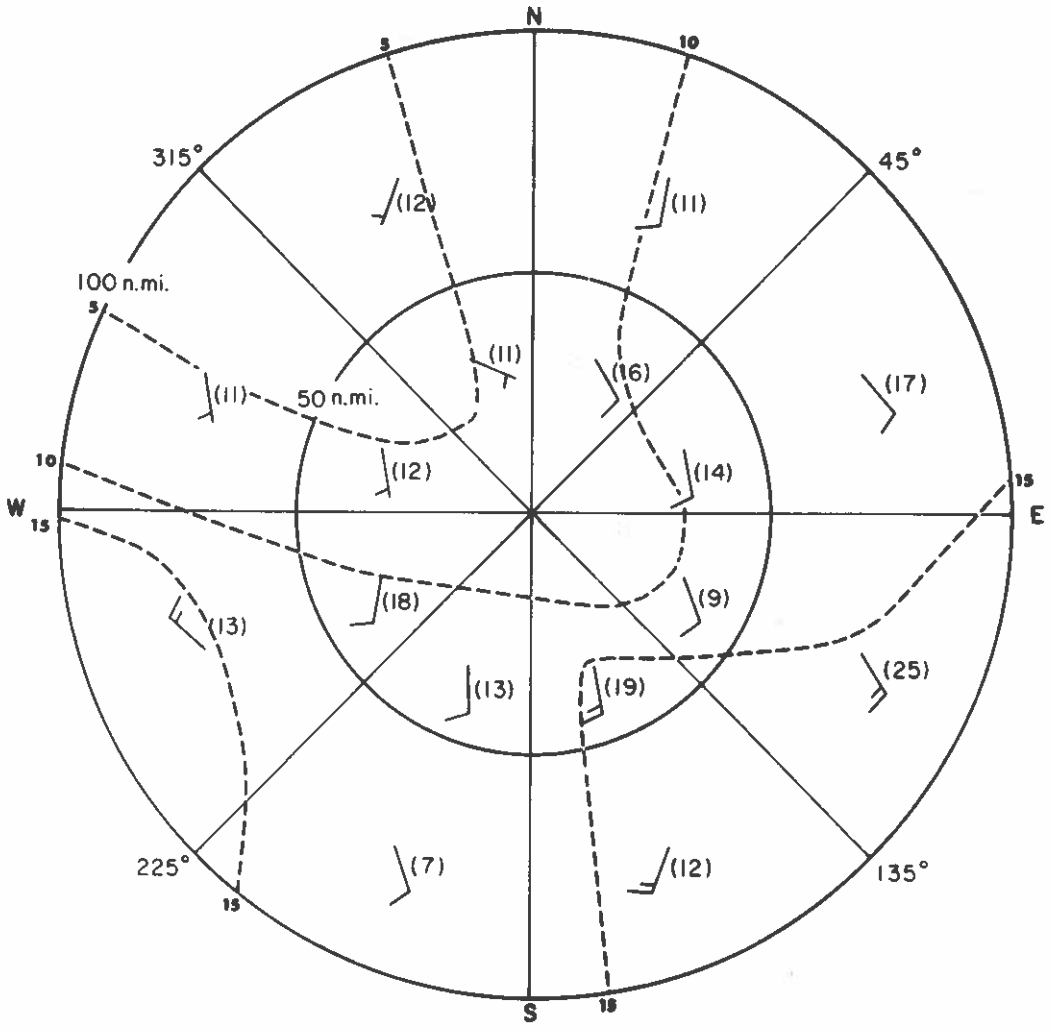

Fig. 7 (above). Composited surface vector winds (in knots) from 220 Great Plains tornado proximity soundings. The center of the circles is the position where the tornado occurred. The figure in parentheses denotes the number of observations which determined the resultant wind in that region. Isotachs are drawn with dashed lines.

Fig. 8 (opposite, upper). Surface divergence pattern (in units of 10^{-6} sec^{-1}) calculated from individual u- and v-component analyses. Circled value at center denotes location of tornado. Regions of maximum divergence are marked DIV, regions of maximum convergence are labeled CON. North is pointing upward.

Fig. 9 (opposite, lower). Surface relative vorticity pattern (in units of 10^{-6} sec^{-1}) calculated from individual u- and v-component analyses. The circled value in the center denotes the location of the tornado. Regions of maximum cyclonic relative vorticity are marked C and regions of anticyclonic vorticity are labeled A. North is pointing upward.

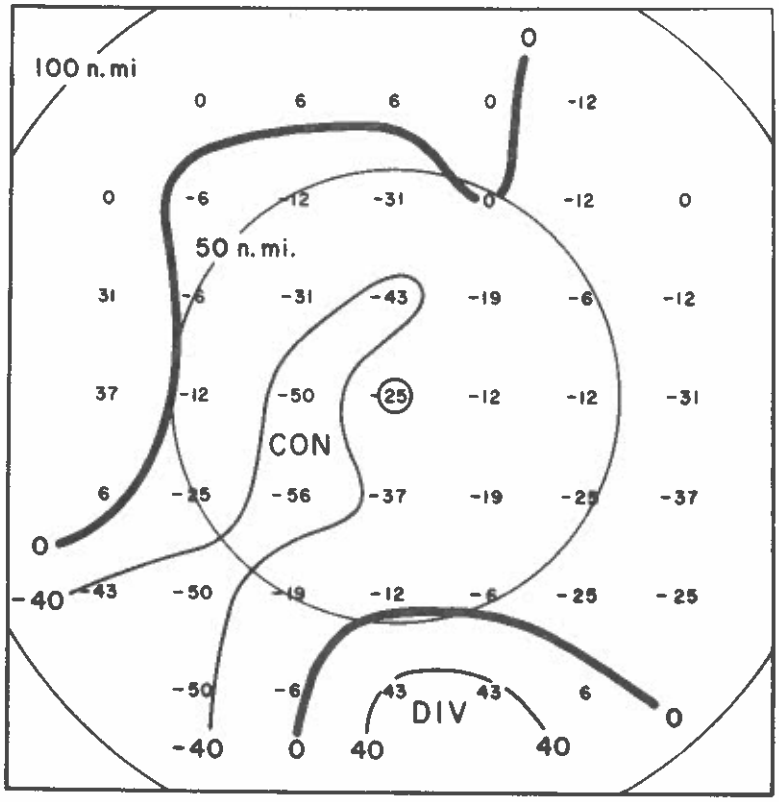
100 n. mi
50 n. mi.
CON
DIV
0
6
6
0
-12
-6
-12
-31
-12
0
31
-6
-31
-43
-19
-6
-12
37
-12
-50
25
-12
-12
-31
6
-25
-56
-37
-19
-25
-37
-40
-43
-50
-19
-12
-6
-25
-25
-50
-6
43
43
6
-40
40
40

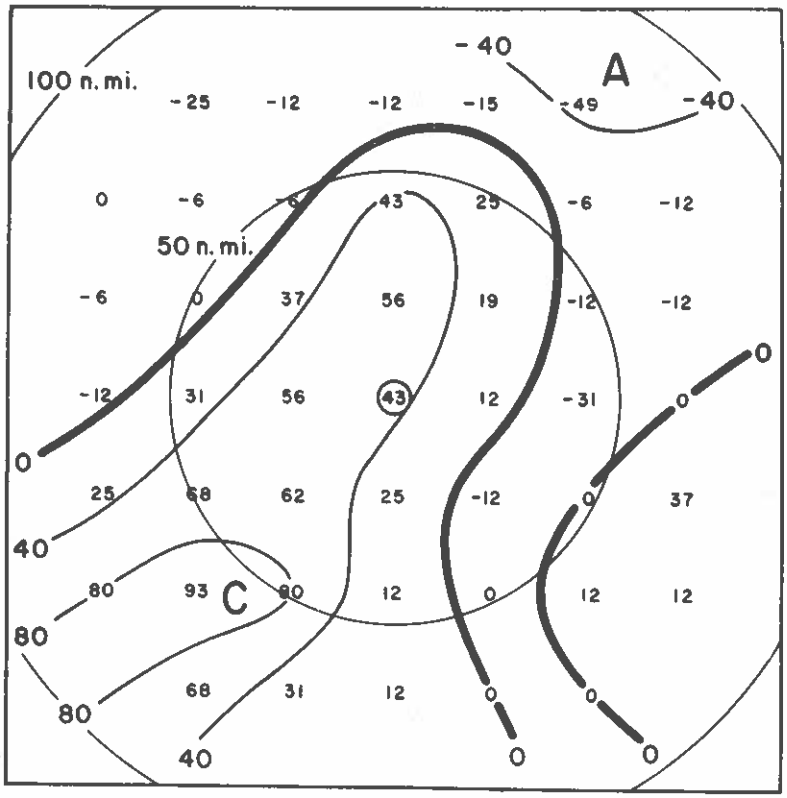
100 n. mi.
50 n. mi.
A
C
-40
-25
-12
-12
-15
-49
-40
0
-6
43
25
-6
-12
-6
0
37
56
19
-12
-12
-12
31
56
43
12
-31
25
68
62
25
-12
37
80
93
80
12
0
12
12
68
31
12
40
80
80
40

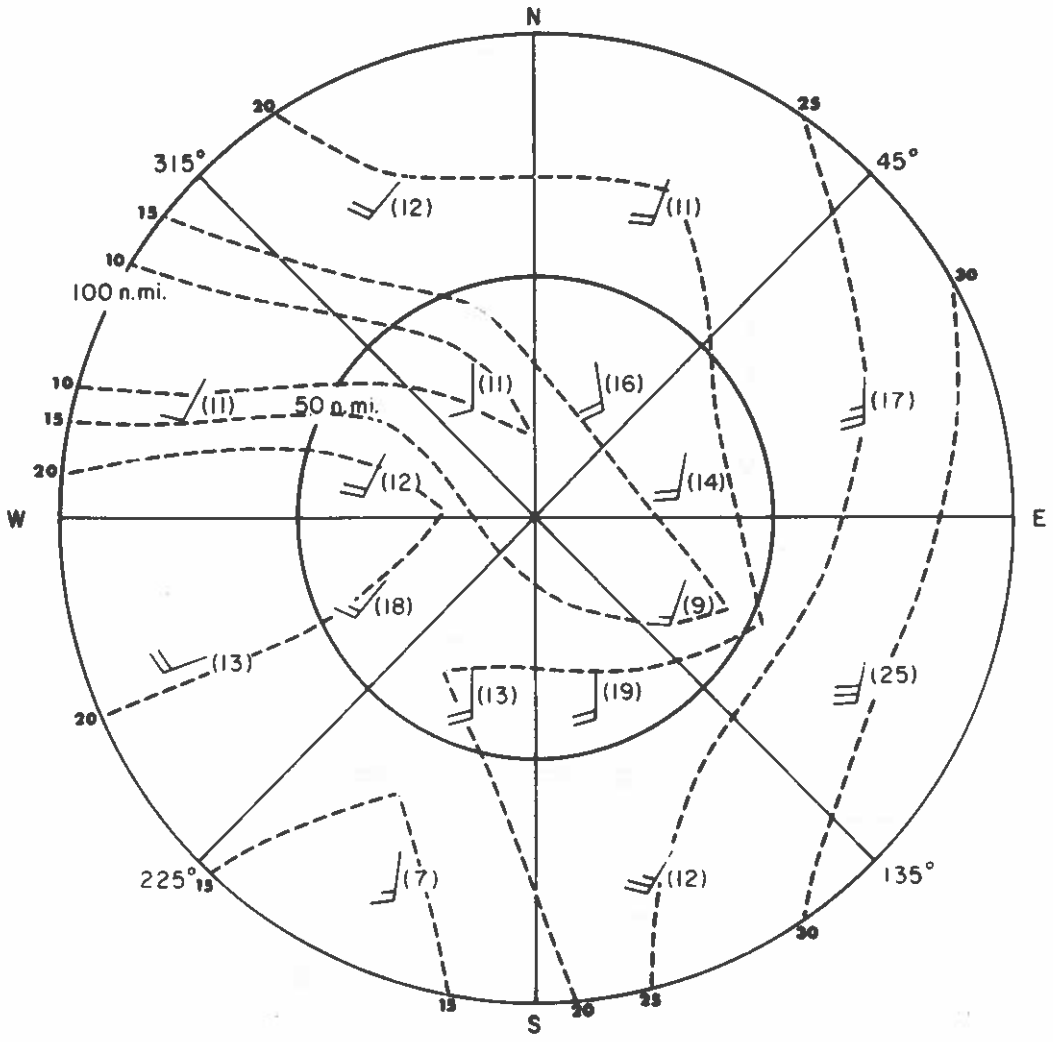

Fig. 10 (above). Composited 850 mb vector winds (in knots) from 220 Great Plains tornado proximity soundings. The center of the circles is the position where the tornado occurred. The figure in parentheses denotes the number of observations which determined the resultant wind in that region. Isotachs are drawn with dashed lines.

Fig. 11 (opposite, upper). 850 mb divergence pattern (in units of 10^{-6} sec^{-1}) calculated from individual u- and v-component analyses. Circled value at center denotes location of tornado. Regions of maximum divergence are marked DIV, regions of maximum convergence are labeled CON. North is pointing upward.

Fig. 12 (opposite, lower). 850 mb relative vorticity pattern (in units of 10^{-6} sec^{-1}) calculated from individual u- and v-component analyses. The circled value in the center denotes the location of the tornado. Regions of maximum cyclonic relative vorticity are marked C and regions of anticyclonic vorticity are labeled A. North is pointing upward.

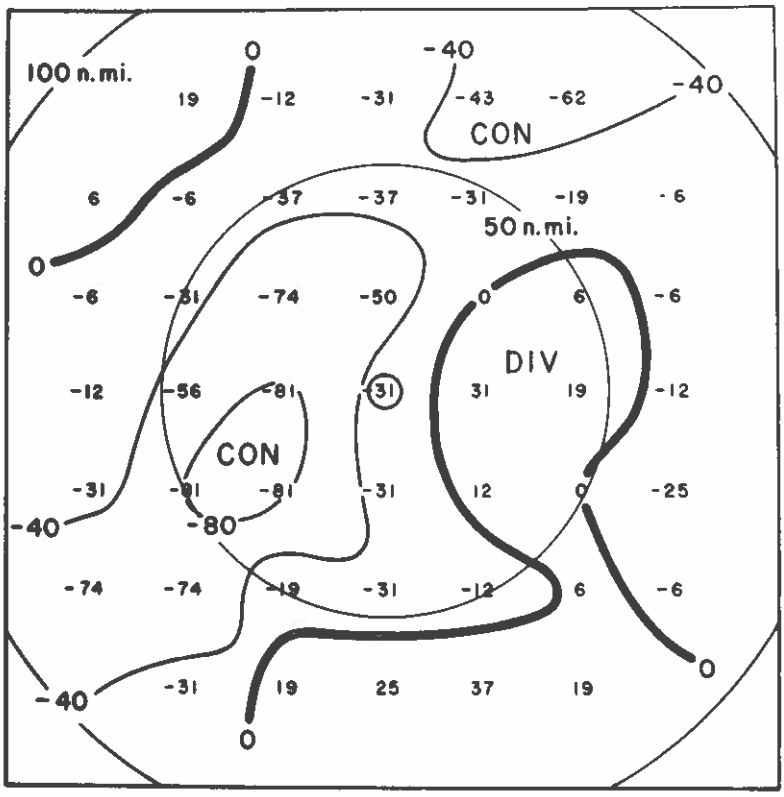
100 n.mi.
0
-40
-40
19
-12
-31
-43
-62
CON
6
-6
-37
-37
-31
-19
-6
50 n.mi.
0
-6
-31
-74
-50
0
6
-6
DIV
-12
-56
-81
31
31
19
-12
CON
-31
-81
-81
-31
12
0
-25
-40
-80
-74
-74
-19
-31
-12
6
-6
-40
-31
19
25
37
19
0
0

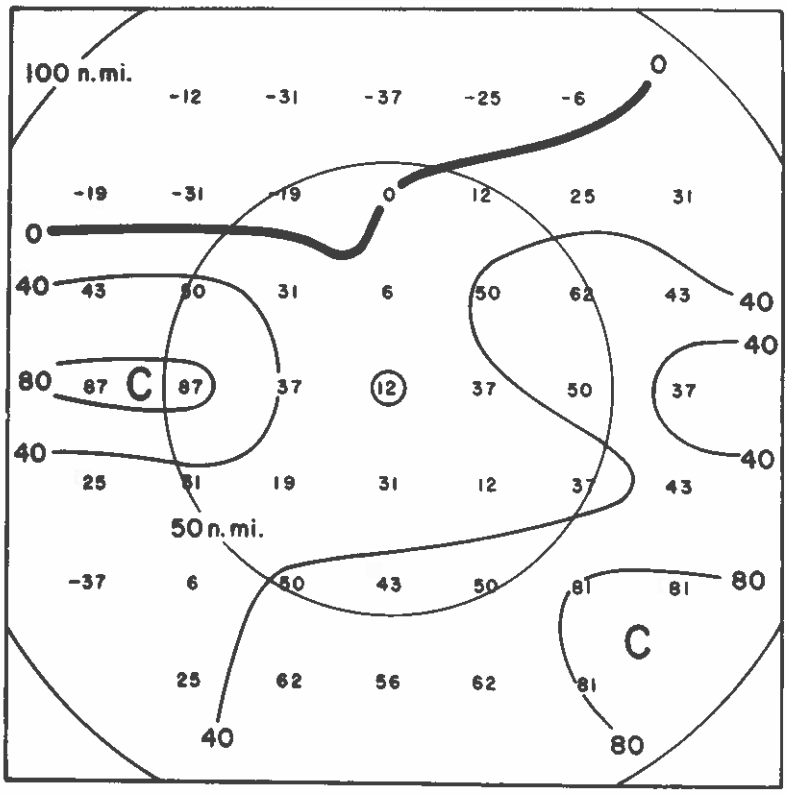
100 n.mi.
0
-12
-31
-37
-25
-6
-19
-31
-19
0
12
25
31
0
40
43
50
31
6
50
62
43
40
40
80
87
C
87
37
12
37
50
37
40
40
25
31
19
31
12
37
43
50 n.mi.
-37
6
50
43
50
81
81
80
C
25
62
56
62
81
40
80

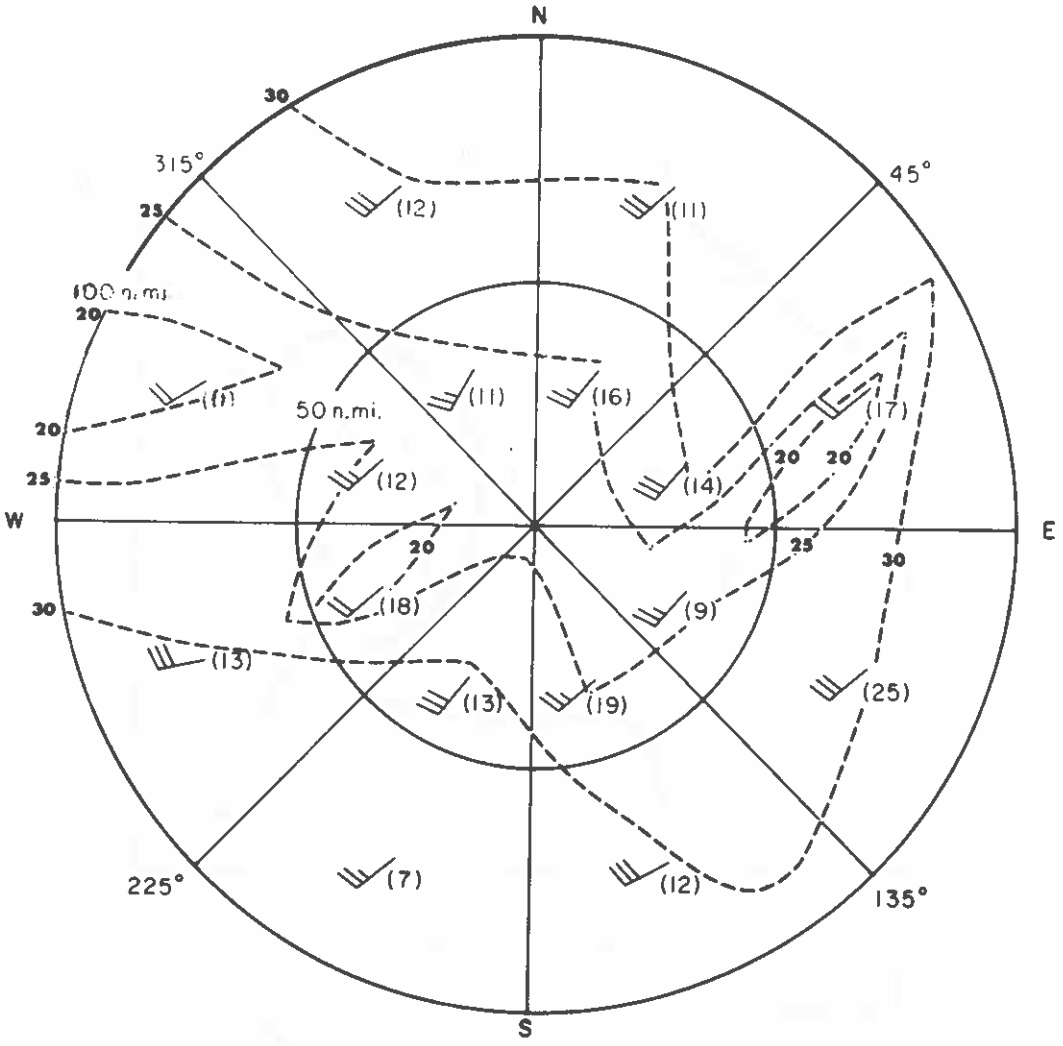

Fig. 13 (above). Composited 700 mb vector winds (in knots) from 220 Great Plains tornado proximity soundings. The center of the circles is the position where the tornado occurred. The figure in parentheses denotes the number of observations which determined the resultant wind in that region. Isotachs are drawn with dashed lines.

Fig. 14 (opposite, upper). 700 mb divergence pattern (in units of 10^{-6} sec^{-1}) calculated from individual u- and v-component analyses. Circled value at center denotes location of tornado. Regions of maximum divergence are marked DIV, regions of maximum convergence are labeled CON. North is pointing upward.

Fig. 15 (opposite, lower). 700 mb relative vorticity pattern (in units of 10^{-6} sec^{-1}) calculated from individual u- and v-component analyses. The circled value in the center denotes the location of the tornado. Regions of maximum cyclonic relative vorticity are marked C and regions of anticyclonic vorticity are labeled A. North is pointing upward.

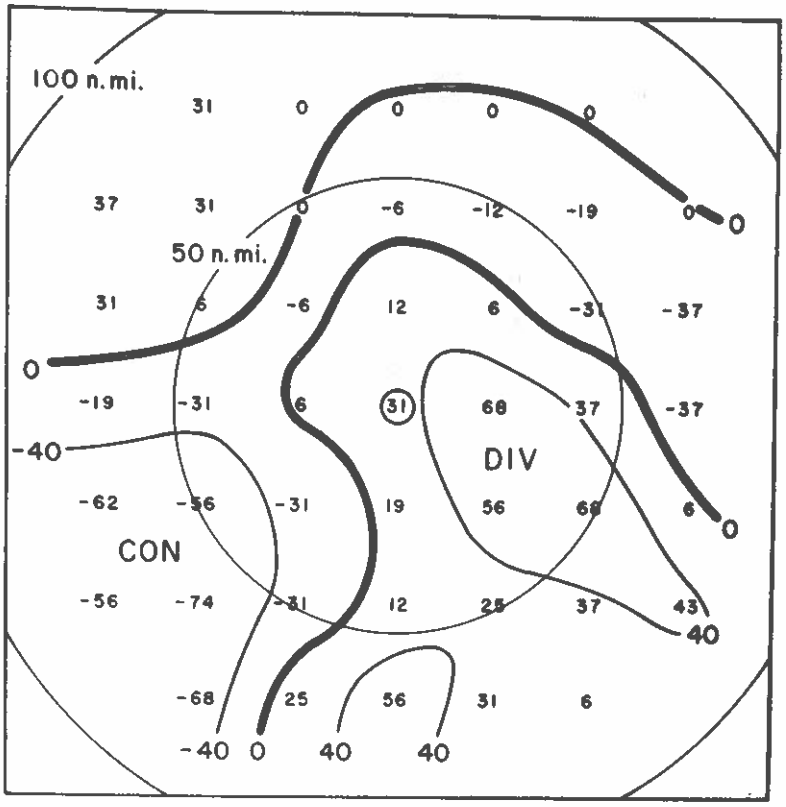
100 n. mi.
50 n. mi.
DIV
CON
31 0 0 0 0
37 31 0 -6 -12 -19 0 0
31 6 -6 12 6 -31 -37
0
-19 -31 6 31 68 37 -37
-40
-62 -56 -31 19 56 68 6 0
-56 -74 -31 12 25 37 43 40
-68 25 56 31 6
-40 0 40 40

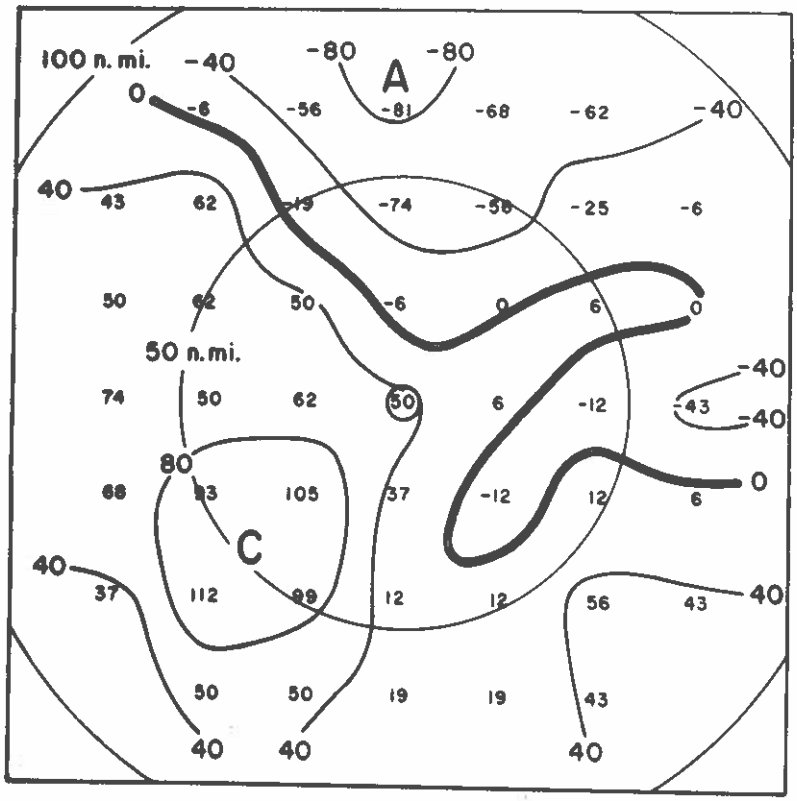
100 n. mi.
50 n. mi.
A
C
-40 -80 -80
0 -6 -56 -81 -68 -62 -40
40 43 62 -19 -74 -56 -25 -6
50 62 50 -6 0 6 0
74 50 62 50 6 -12 -43 -40
80 -40
68 93 105 37 -12 12 6 0
40 37 112 99 12 12 56 43 40
50 50 19 19 43
40 40 40

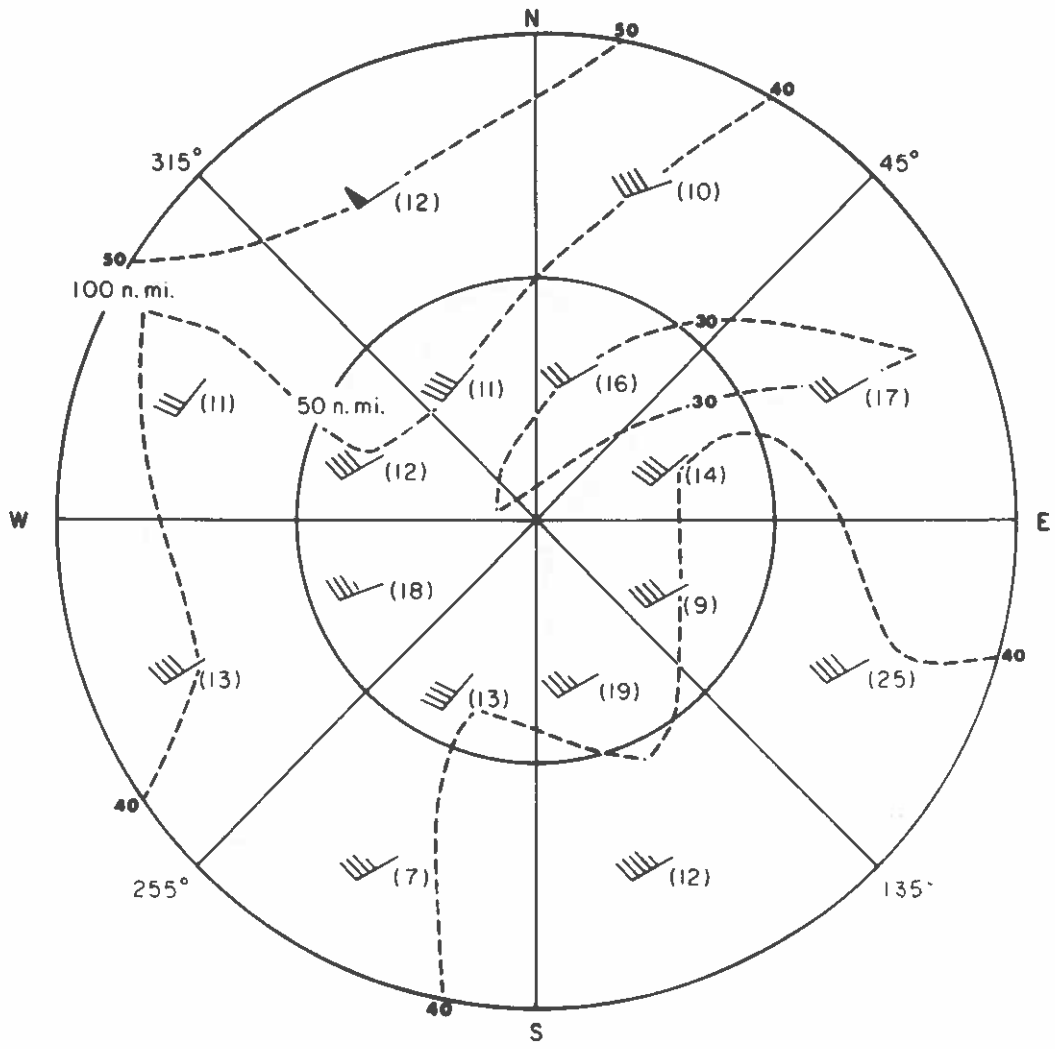

Fig. 16 (above). Composited 500 mb vector winds (in knots) from 220 Great Plains tornado proximity soundings. The center of the circles is the position where the tornado occurred. The figure in parentheses denotes the number of observations which determined the resultant wind in that region. Isotachs are drawn with dashed lines.

Fig. 17 (opposite, upper). 500 mb divergence pattern (in units of 10^{-6} sec^{-1}) calculated from individual u- and v-component analyses. Circled value at center denotes location of tornado. Regions of maximum divergence are marked DIV, regions of maximum convergence are labeled CON. North is pointing upward.

Fig. 18 (opposite, lower). 500 mb relative vorticity pattern (in units of 10^{-6} sec^{-1}) calculated from individual u- and v-component analyses. The circled value in the center denotes the location of the tornado. Regions of maximum cyclonic relative vorticity are marked C and regions of anticyclonic vorticity are labeled A. North is pointing upward.

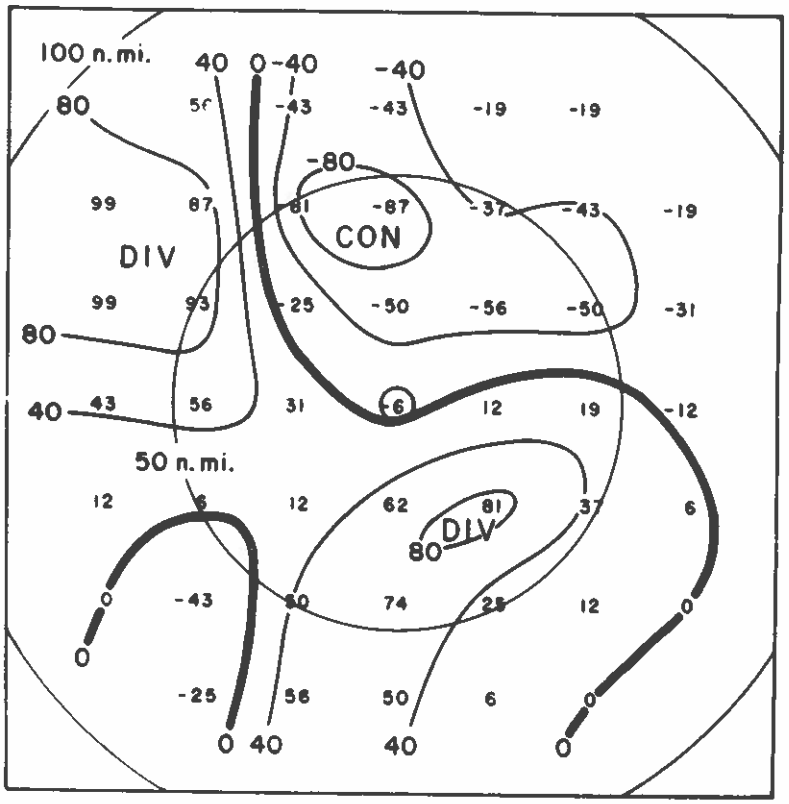
100 n.mi.
50 n.mi.
DIV
CON
DIV

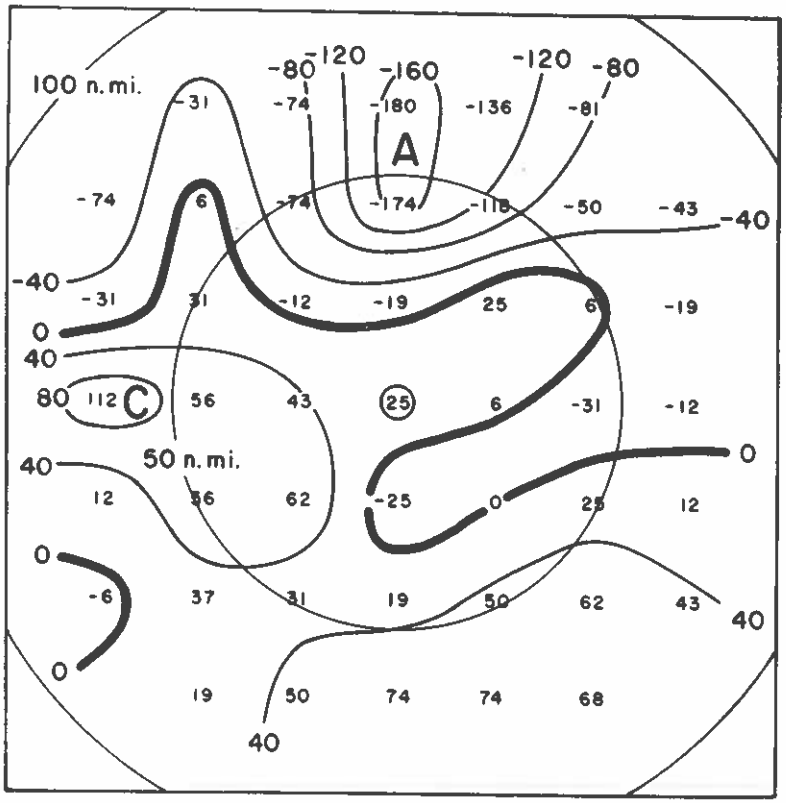
100 n.mi.
50 n.mi.
A
C

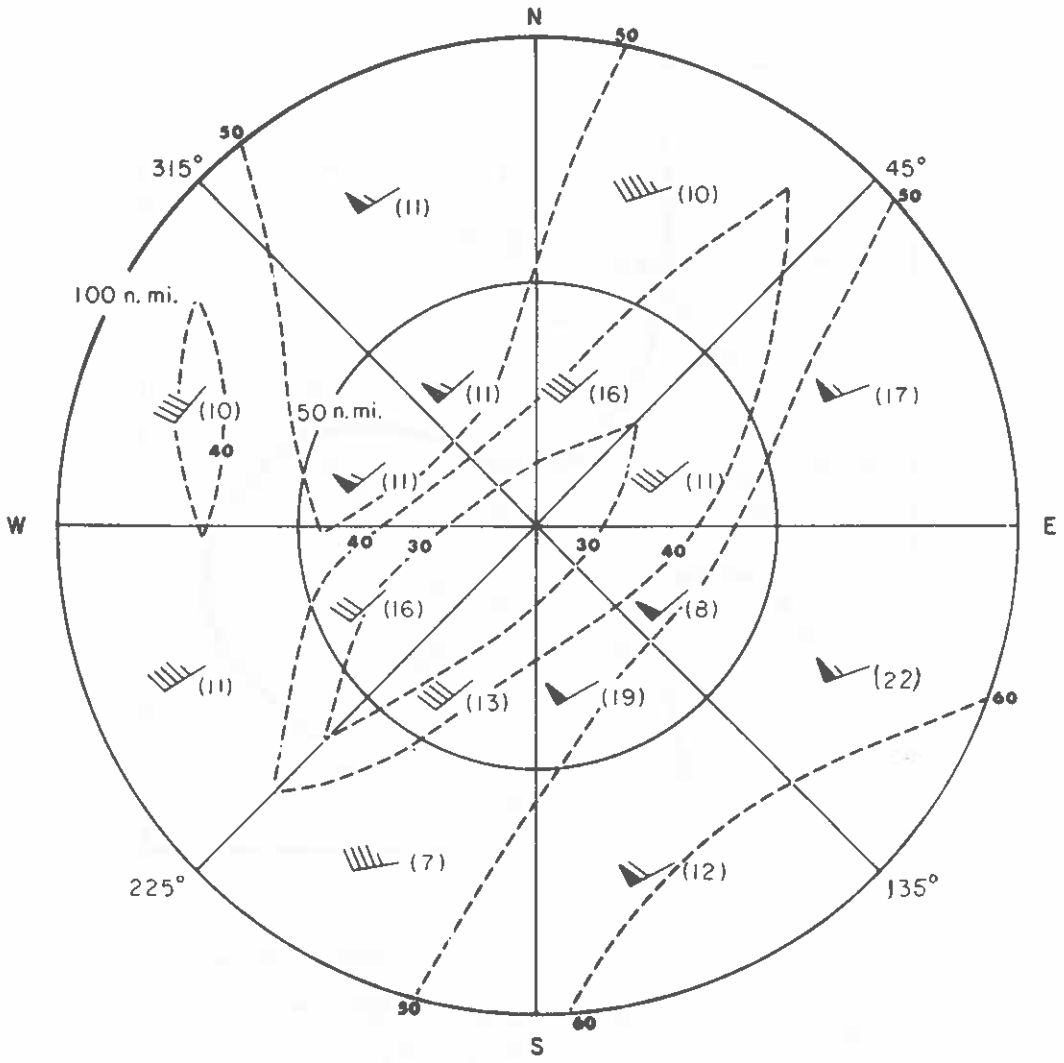

Fig. 19 (above). Composited 300 mb vector winds (in knots) from 220 Great Plains tornado proximity soundings. The center of the circles is the position where the tornado occurred. The figure in parentheses denotes the number of observations which determined the resultant wind in that region. Isotachs are drawn with dashed lines.

Fig. 20 (opposite, upper). 300 mb divergence pattern (in units of 10^{-6} sec^{-1}) calculated from individual u- and v-component analyses. Circled value at center denotes location of tornado. Regions of maximum divergence are marked DIV, regions of maximum convergence are labeled CON. North is pointing upward.

Fig. 21 (opposite, lower). 300 mb relative vorticity pattern (in units of 10^{-6} sec^{-1}) calculated from individual u- and v-component analyses. The circled value in the center denotes the location of the tornado. Regions of maximum cyclonic relative vorticity are marked C and regions of anticyclonic vorticity are labeled A. North is pointing upward.

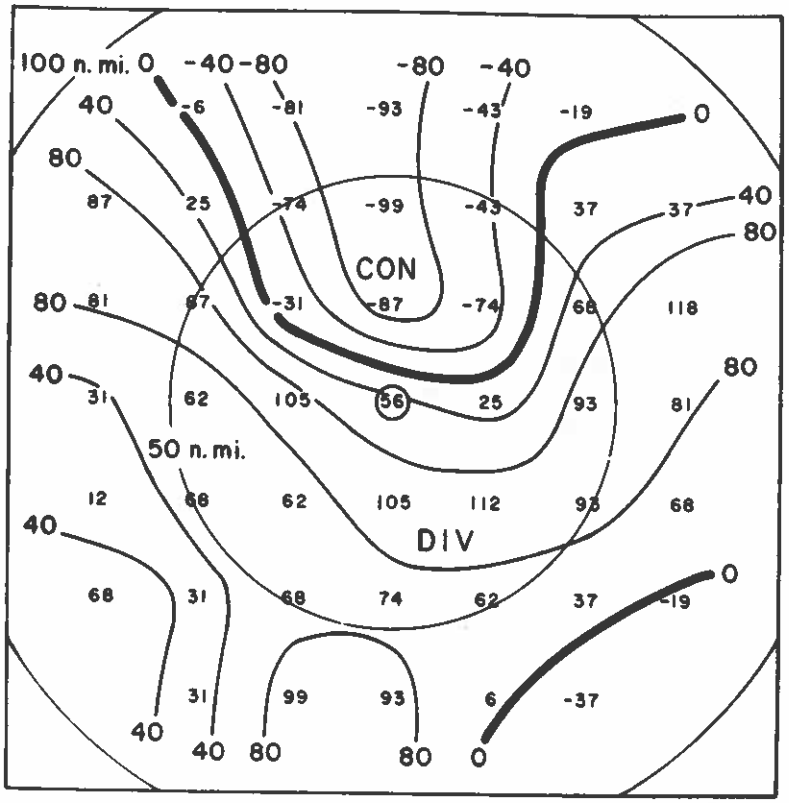
100 n. mi.
CON
DIV
50 n. mi.

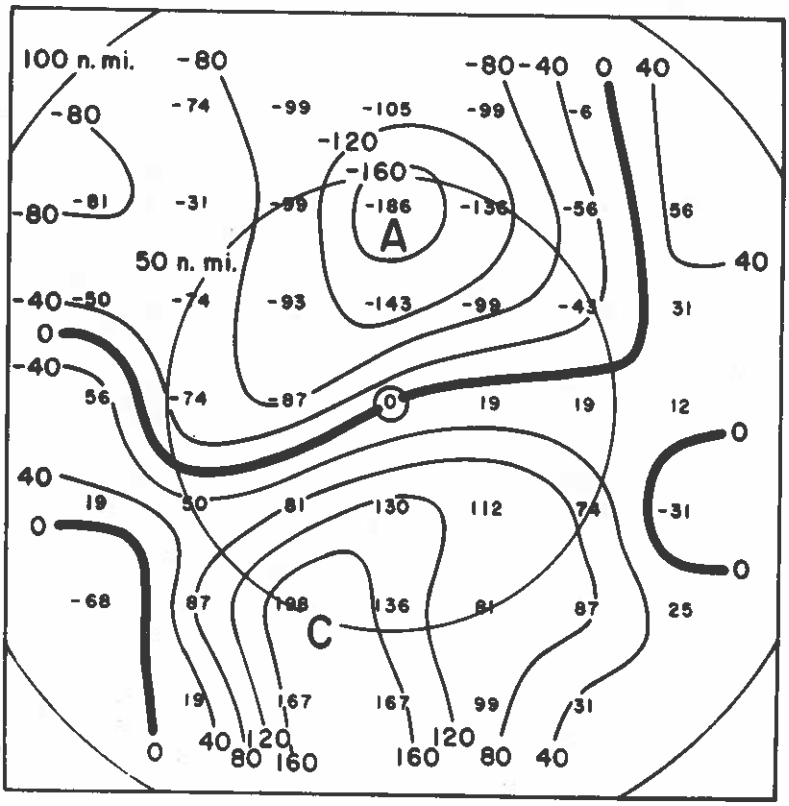
100 n. mi.
A
C
50 n. mi.

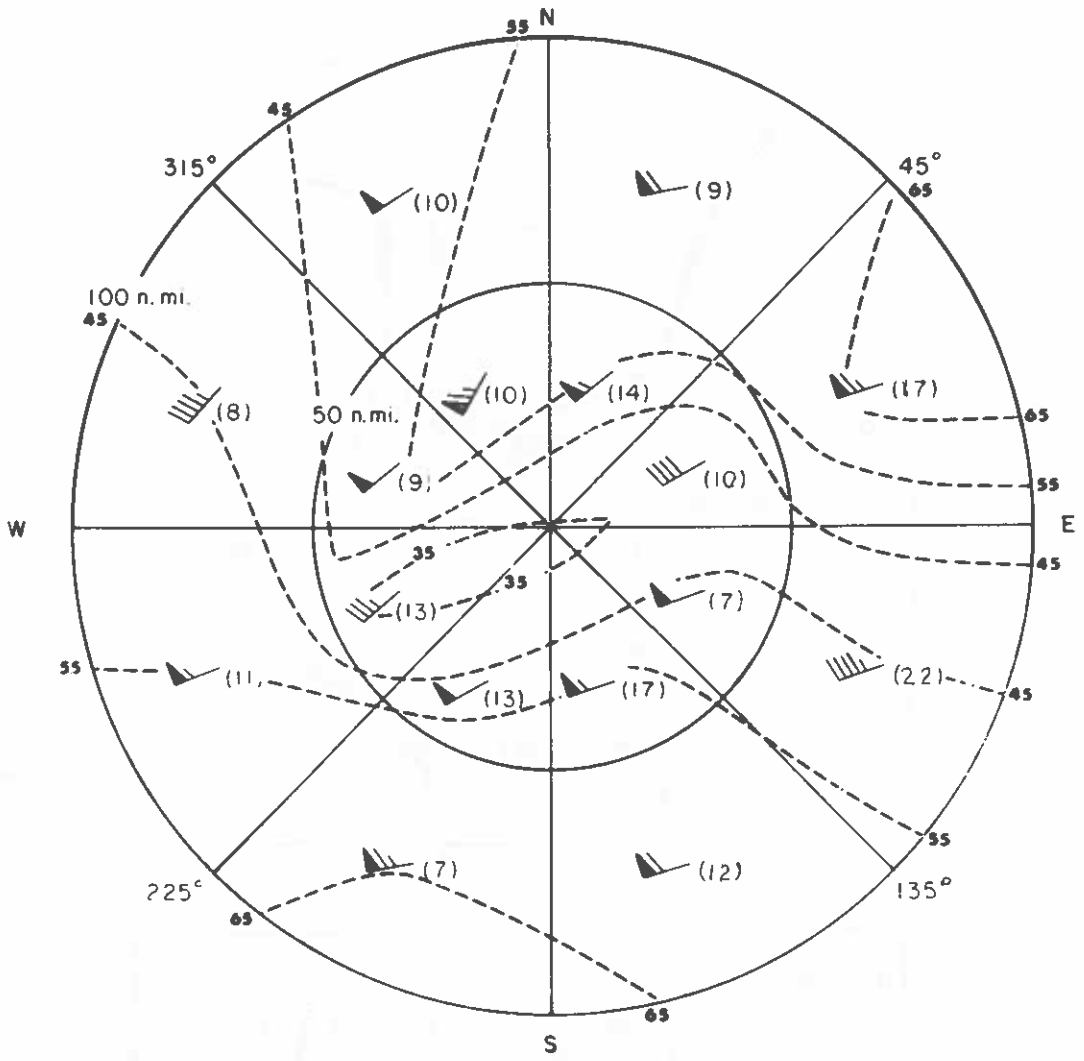

Fig. 22 (above). Composited 200 mb vector winds (in knots) from 220 Great Plains tornado proximity soundings. The center of the circles is the position where the tornado occurred. The figure in parentheses denotes the number of observations which determined the resultant wind in that region. Isotachs are drawn with dashed lines.

Fig. 23 (opposite, upper). 200 mb divergence pattern (in units of 10^{-6} sec^{-1}) calculated from individual u- and v-component analyses. Circled value at center denotes location of tornado. Regions of maximum divergence are marked DIV, regions of maximum convergence are labeled CON. North is pointing upward.

Fig. 24 (opposite, lower). 200 mb relative vorticity pattern (in units of 10^{-6} sec^{-1}) calculated from individual u- and v-component analyses. The circled value in the center denotes the location of the tornado. Regions of maximum cyclonic relative vorticity are marked C and regions of anticyclonic vorticity are labeled A. North is pointing upward.

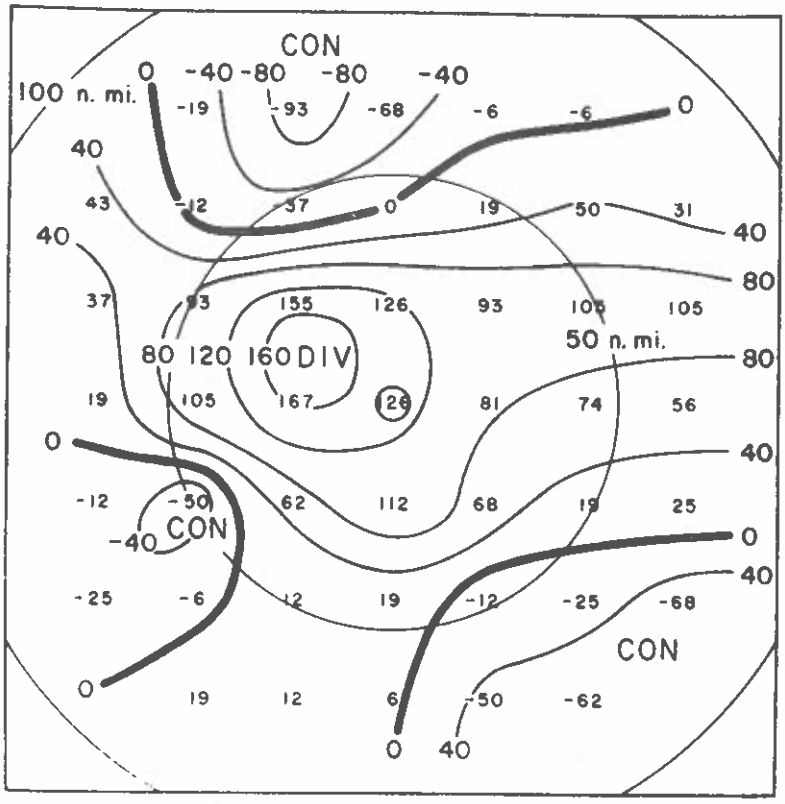
CON
100 n. mi.
0 -40 -80 -80 -40
-19 -93 -68 -6 -6 0
40
43 -12 37 0 19 50 31 40
40
80
37 93 155 126 93 105 105
50 n. mi.
80 120 160 DIV
80
19 105 167 126 81 74 56
0
40
-12 -50 62 112 68 19 25
-40 CON
0
40
-25 -6 12 19 -12 -25 -68
CON
0 19 12 6 -50 -62
0 40

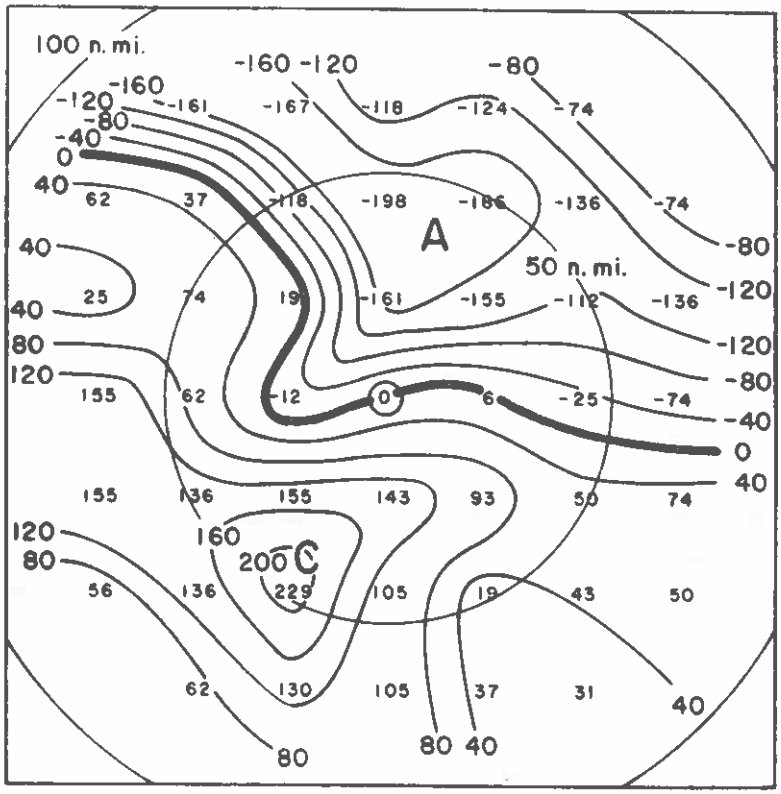
100 n. mi.
-160 -120 -80
-160
-120 -161 -167 -118 -124 -74
-80
-40
0
40 62 37 -118 -198 -186 -136 -74
A
40
50 n. mi.
-80
40 25 74 19 -161 -155 -112 -136 -120
80
-120
120
-80
155 62 -12 0 6 -25 -74
-40
0
40
155 136 155 143 93 50 74
120
160
80
200 C
56 136 225 105 19 43 50
62 130 105 37 31
40
80
80 40

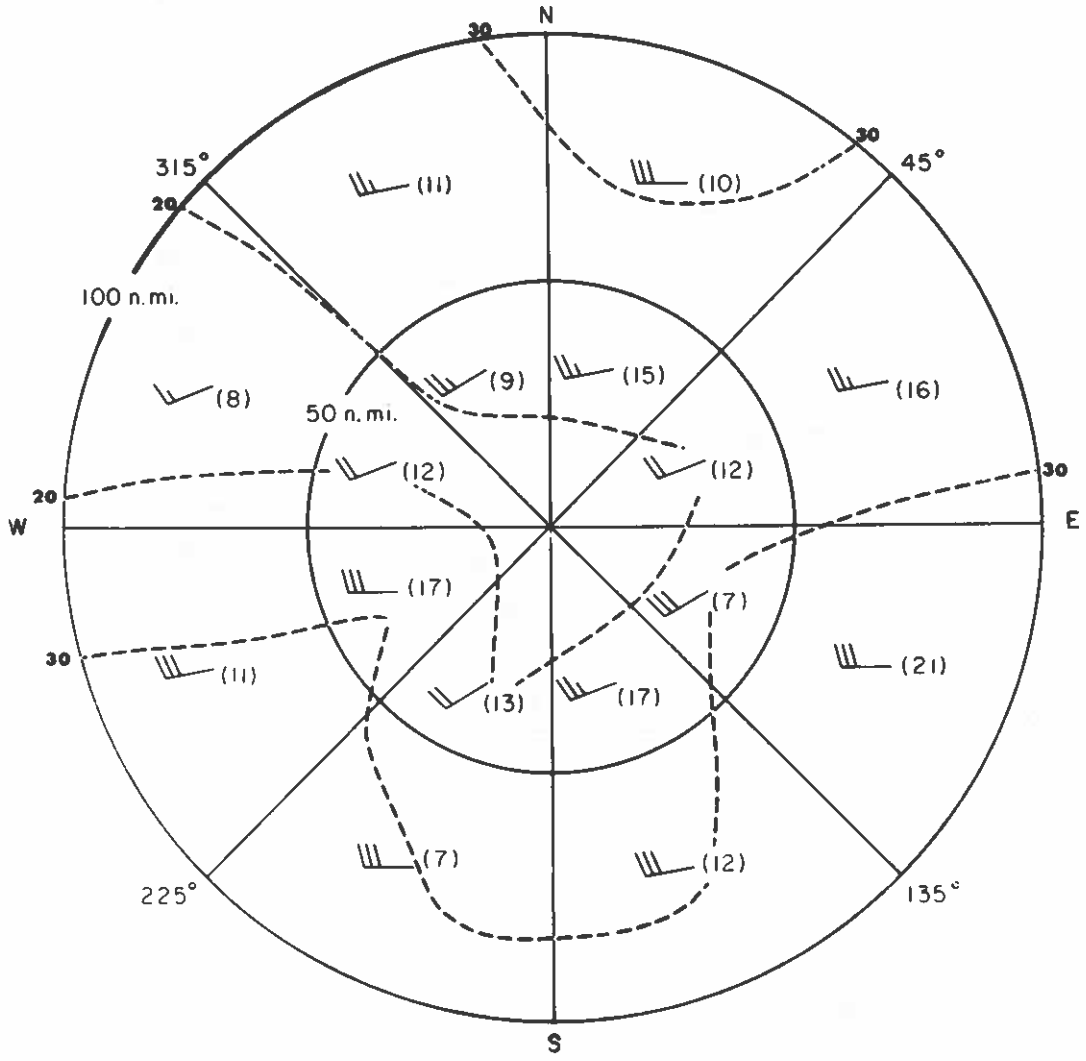

Fig. 25. Composited 100 mb vector winds (in knots) from 220 Great Plains tornado proximity soundings. The center of the circles is the position where the tornado occurred. The figure in parentheses denotes the number of observations which determined the resultant wind in that region. Isotachs are drawn with dashed lines.

blocking effect created by cumulonimbus clouds in large vertically shearing flow would lend credence to the thunderstorm theories of Newton and Newton (op. cit.) and Fujita and Grandoso (op. cit.) and to the tornado formation theories of Markgraf (op. cit.), Wegener (op. cit.), Bates (op. cit.) and Gray (op. cit.).

Relative Vorticity and Divergence Fields Derived from the Composited Winds

From the u- and v-components of the composited tornado environment winds, divergence and relative vorticity analyses were made for each standard level up to 200 mb. The divergence analyses are shown in Figs. 8, 11, 14, 17, 20, and 23. The relative vorticity analyses are shown in Figs. 9, 12, 15, 18, 21, and 24.

There were major differences between the upper and lower tropospheric levels in these kinematic components. At 850 mb, the relative vorticity is positive over most of the region. The strongest regions of convergence and positive relative vorticity are found to the west of the tornado center. The order of magnitude of the divergence and relative vorticity ($\sim 100 \times 10^{-6} sec^{-1}$) is large by synoptic scale standards, but an order of magnitude less than values presented for mesoscale analyses (Fujita and Grandoso, op. cit.) and several orders of magnitude less than values calculated by Hoecker (1960) in his microscale analysis of the Dallas tornado.

Two extreme regimes of relative vorticity can be noted at 200 mb. A region of strong positive relative vorticity is present to

the upwind right of the tornado. A region of equally strong negative relative vorticity is located downwind and to the left of the center.

The divergence pattern at 200 mb shows weak convergence upstream and to the far right and left of the center of the tornado. A large strong divergence region is observed beginning a few miles upstream of the center and extending far downstream. These relative vorticity and divergence patterns are believed to follow as a direct consequence of blocking of the mean wind field by cumulonimbus clouds.

Vertical Profiles of Divergence and Relative Vorticity

To more explicitly portray these divergence and convergence patterns in relation to the surrounding wind fields, a natural coordinate system was adopted. The axis of this natural coordinate system was chosen as a line from 240° to 060° azimuth angle (the direction of the mean upper level wind field). Only data points within a 50-mile radius of the center were considered. The maximum value of relative vorticity and divergence to the right and left of the center of the coordinate system were used at each level to construct vertical profiles of these parameters.

Fig. 26 shows that to the right of the storm center the relative vorticity is positive at all levels. The magnitude of vorticity increases from a minimum at the surface to a maximum at 200 mb. The relative vorticity to the left of the center is positive in the lower

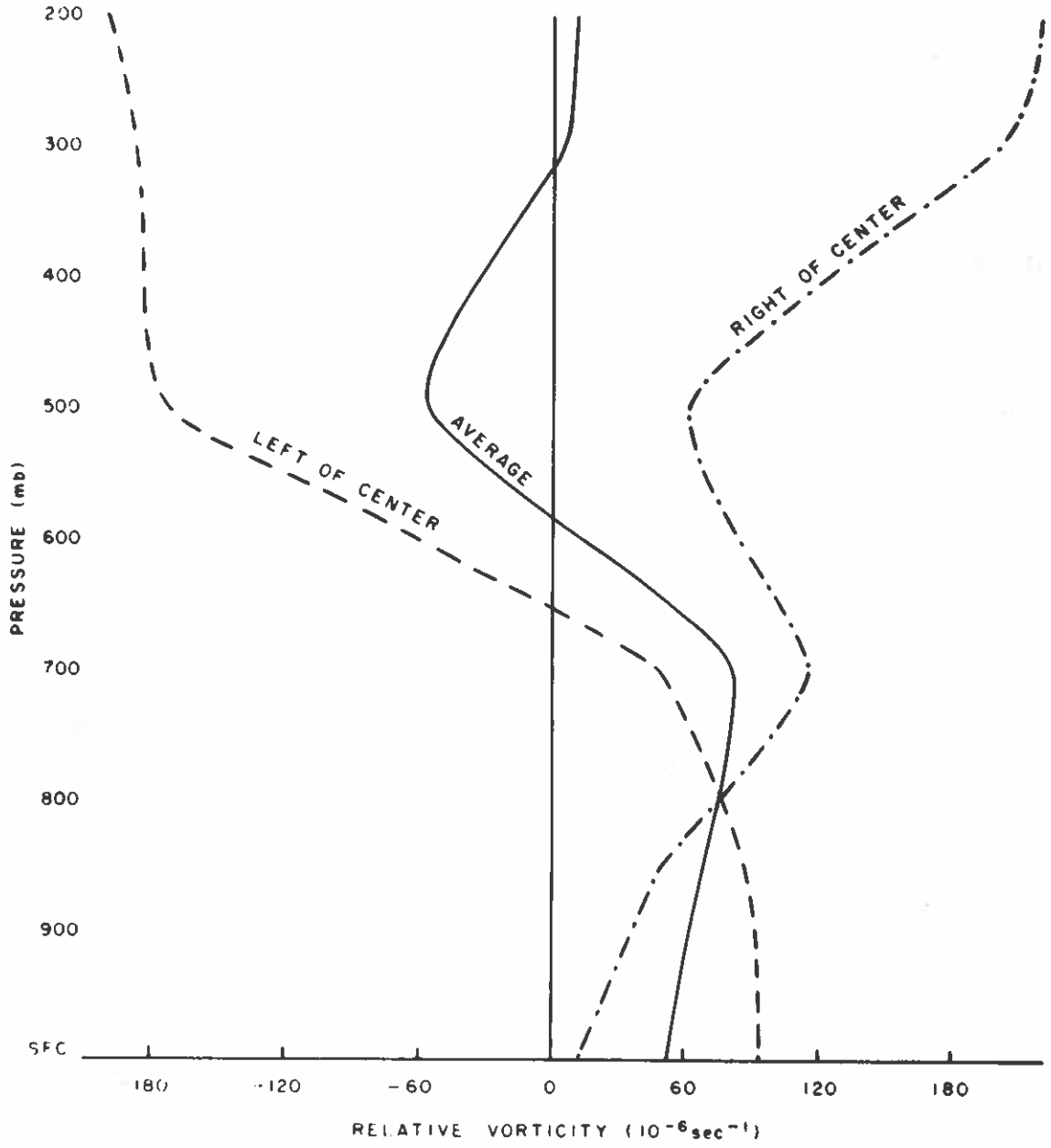

Fig. 26. Vertical profiles of relative vorticity plotted from maximum values to the right and left of center of a natural coordinate system looking downstream along the mean upper level wind and oriented along the 240° to 060° direction.

levels and then is observed to be strongly negative at upper levels. The average of these two profiles shows strong positive relative vorticity in the lower levels, weak negative vorticity at 500 mb, and a region of nearly zero relative vorticity in the upper troposphere. These average profiles show that calculations made from averaging around the tornado environment are very misleading. Two distinct wind flow fields exist in the tornado environment due to the apparent blocking action of the large cumulonimbi. The existence of a "blocked" wind field produced by cumulonimbus clouds should be included in any discussion of the tornado environment.

Fig. 27 portrays the profile of divergence. To the right of center, convergence appears at the surface, but steadily increasing values of divergence are noted with height above the surface. The profile to the left of center shows strong convergence at all levels except 700 mb and 200 mb.

The divergence and relative vorticity analyses were next separated into quadrants relative to the mean upper wind field. This was done by constructing a line (from 330° to 150° azimuth angle) perpendicular to the axis of the natural coordinate system at the tornado's center. Average values of divergence and relative vorticity were computed in each of these quadrants and vertical profiles were determined (Figs. 28, 29, 30, and 31).

These quadrant vertical profiles aid in describing the three-dimensional flow patterns within the tornado environment. Air

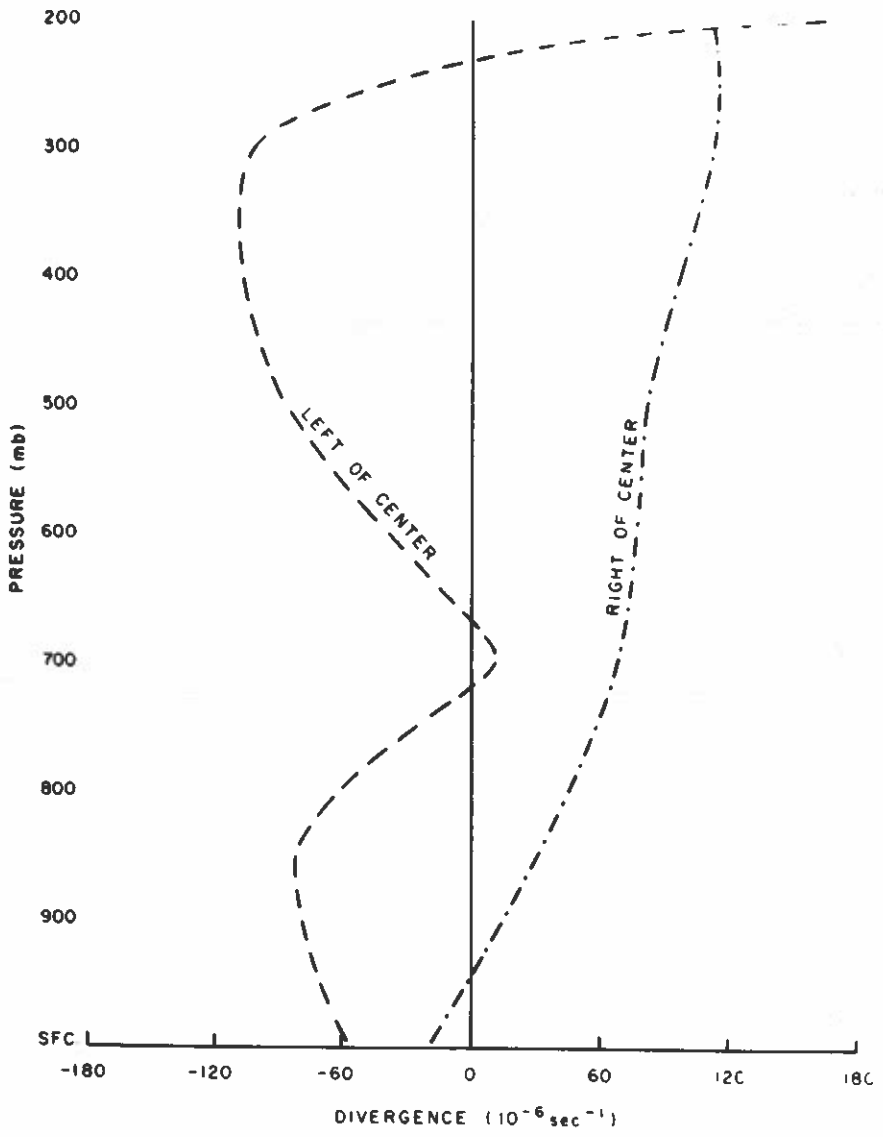

Fig. 27. Vertical profiles of divergence plotted from maximum values to the right and left of center of a natural coordinate system looking downstream along the mean upper level wind and oriented along the 240° to 060° direction.

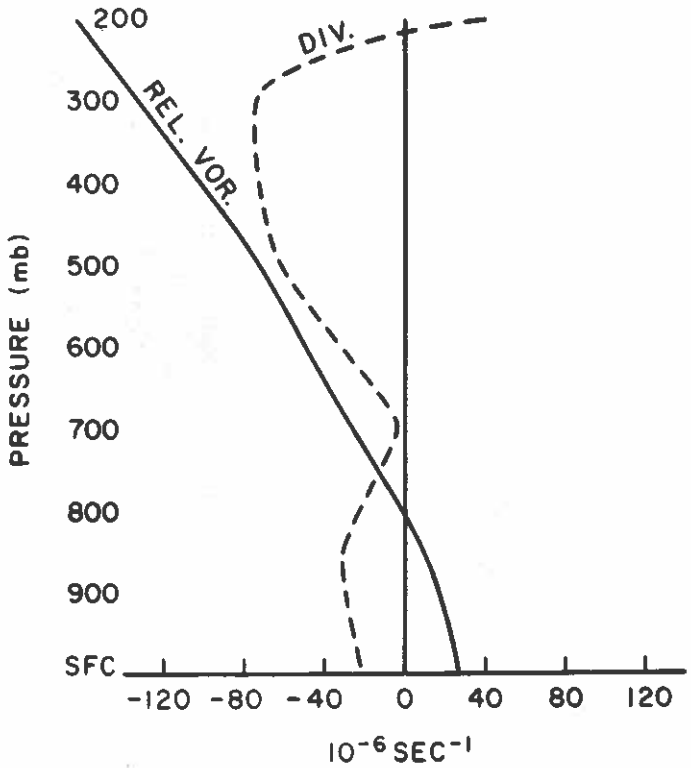

Fig. 28. Average vertical profiles of tornado environment relative vorticity and divergence for the left front quadrant relative to a coordinate system oriented along the 240° to 060° azimuth direction and centered on the tornado location. The left front quadrant includes the area from azimuth directions 330° to 060°.

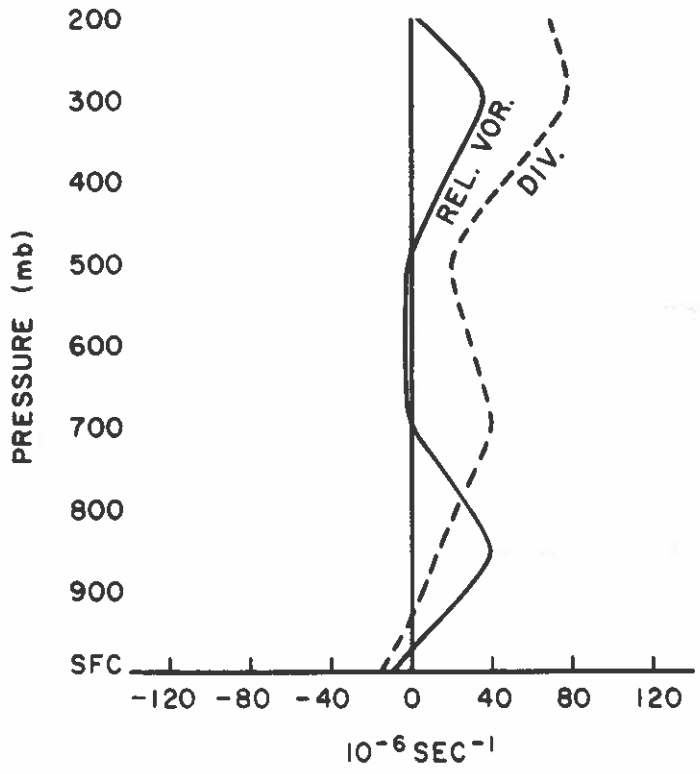

Fig. 29. Average vertical profiles of tornado environment relative vorticity and divergence for the right front quadrant relative to a coordinate system oriented along the 240° to 060° azimuth direction and centered on the tornado location. The right front quadrant includes the area from azimuth directions 060° to 150°.

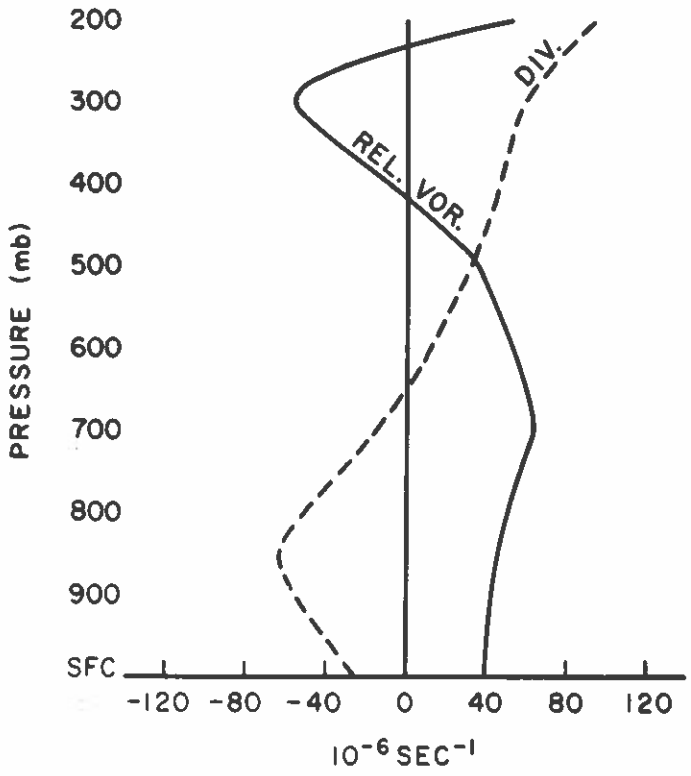

Fig. 30. Average vertical profiles of tornado environment relative vorticity and divergence for the left rear quadrant relative to a coordinate system oriented along the 240° to 060° azimuth direction and centered on the tornado location. The left rear quadrant includes the area from azimuth directions 240° to 330°.

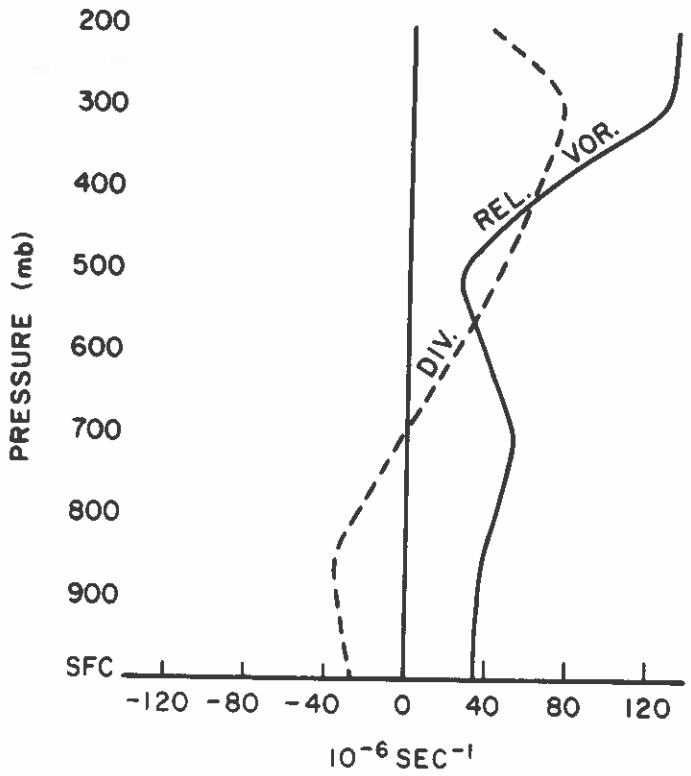

Fig. 31. Average vertical profiles of tornado environment relative vorticity and divergence for the right rear quadrant relative to a coordinate system oriented along the 240° to 060° azimuth direction and centered on the tornado location. The right rear quadrant includes the area from azimuth directions 150° to 240°.

approaching the tornado at low levels possesses positive relative vorticity and is converging. At upper levels the approaching air has positive vorticity but is undergoing strong divergence. Downwind from the position of the tornado a very different pattern is observed at upper levels while the lower level flow is essentially the same. At upper levels, air which has passed to the left of the blocking cumulonimbus is strongly convergent and has very strong anticyclonic relative vorticity. Air which has traveled to the right of the block possesses weak cyclonic relative vorticity and is strongly divergent.

It was not expected that such clearly different divergent and convergent patterns would have been observed at upper levels to the right and left of the tornado center.

IV. OBSERVED TORNADO ENVIRONMENT CUMULUS POTENTIAL BUOYANCY

The equivalent potential temperature (θ_e) was calculated at each standard level from the sounding data. A parameter, cumulus potential buoyancy (CPB), was then defined as a measure of the vertical instability of the atmosphere. This parameter was defined as the magnitude of the decrease of θ_e from the surface to its lowest value below 500 mb. Similar calculations involving θ_e have been discussed by other researchers, particularly Darkow (op. cit.) who established what he calls a Total Energy Index.

θ_e vertical profiles for the four geographical regions and the mean for all cases are shown in Fig. 32. These θ_e profiles were constructed from only those soundings which were definitely known to have been in the warm moist air mass preceding tornado formation. Large cumulus potential buoyancy exists for all cases and the geographical differences are not large or surprising. The Northeastern profile is noticeably colder than the others at all levels while the Great Plains exhibit the greatest mean cumulus potential buoyancy. The very high surface θ_e shown by the Great Plains data is primarily a result of terrain elevation.

The cumulus potential buoyancy (CPB) values resulting from the vertical profiles of Fig. 32 are probably not as large as CPB values at the actual time and place of tornado genesis. Local "hot (and moist) spots," due to differing types of vegetation, elevated

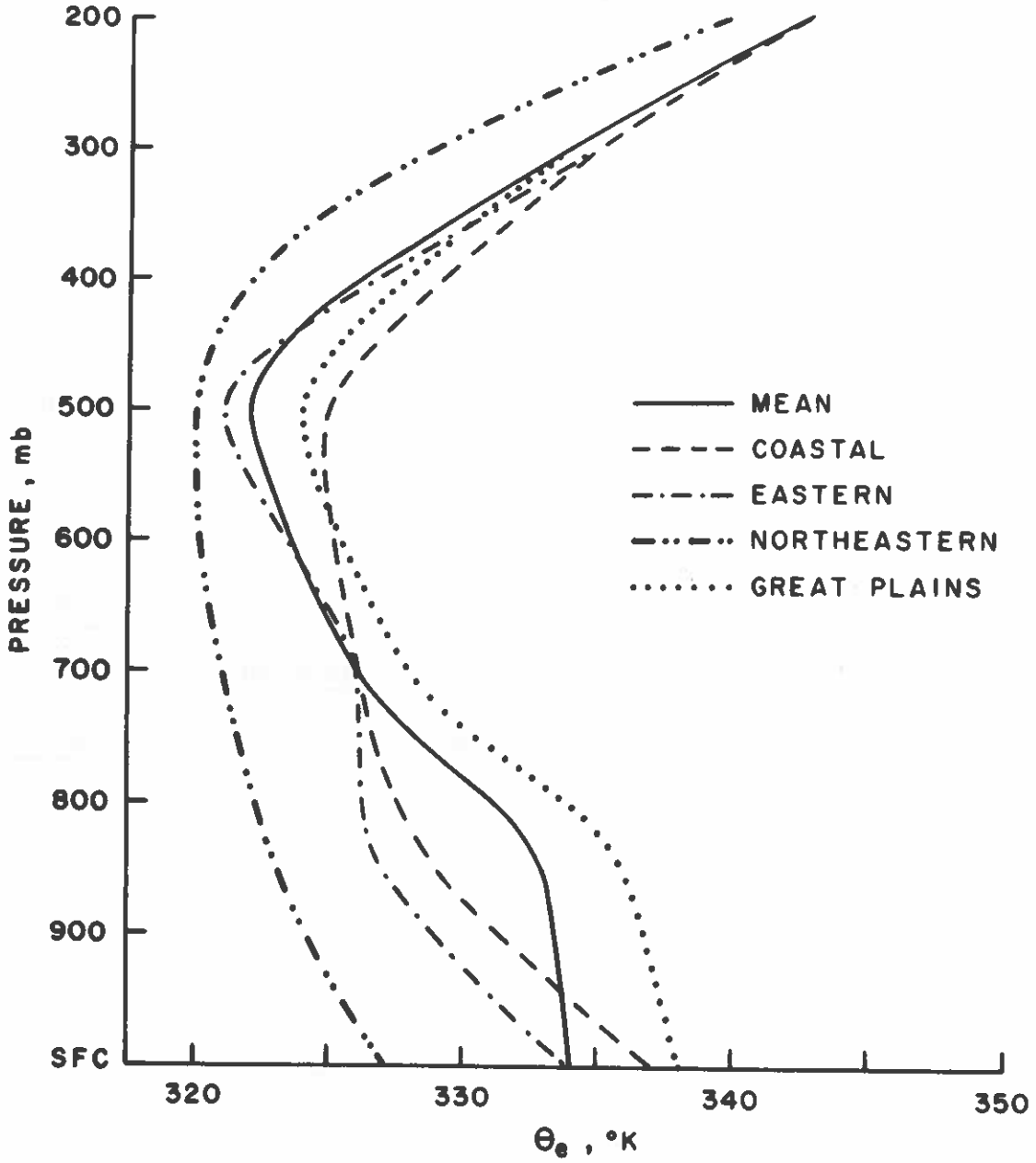

Fig. 32. Average vertical θ_e profiles for the various geographical regions and the mean for all warm air mass cases.

terrain, and other factors are readily noted in mesoscale analyses, but not from synoptically spaced radiosonde data. Since only a 1° C increase in surface temperature and dew point produces a 3° C increase of θ_e, these local "hot (or moist) spots" most definitely exhibit far greater cumulus potential buoyancy than is evidenced from the profiles of Fig. 32.

Comparison of Tropical Storm and Non-Tropical Storm θ_e Profiles

The mean θ_e profile of the warm air mass cases and the θ_e profile for the tropical storm induced tornado cases are shown by Fig. 33. Due to the probable greater mixing and homogeneity of the tropical storm air mass, CPB values cannot be assumed to be appreciably stronger in local regions due to "hot (or moist) spots." This apparent lack of large cumulus potential buoyancy for the tropical storm induced tornadoes was not expected.

Previous studies of tropical storm induced tornadoes [Hill, Malkin, and Schultz (1966), Pearson and Sadowski (1965), and Goldstein (1968)] have not pointed out the cumulus potential buoyancy differences between the tropical storm and non-tropical storm induced tornadoes. The widely used severe weather forecasting indices [Showalter (op. cit.), Galway (op. cit.), Miller, Waters, and Bartlett (op. cit.), and Darkow (op. cit.)] all fail to indicate a potential for severe weather when used with the mean tropical storm induced tornado soundings.

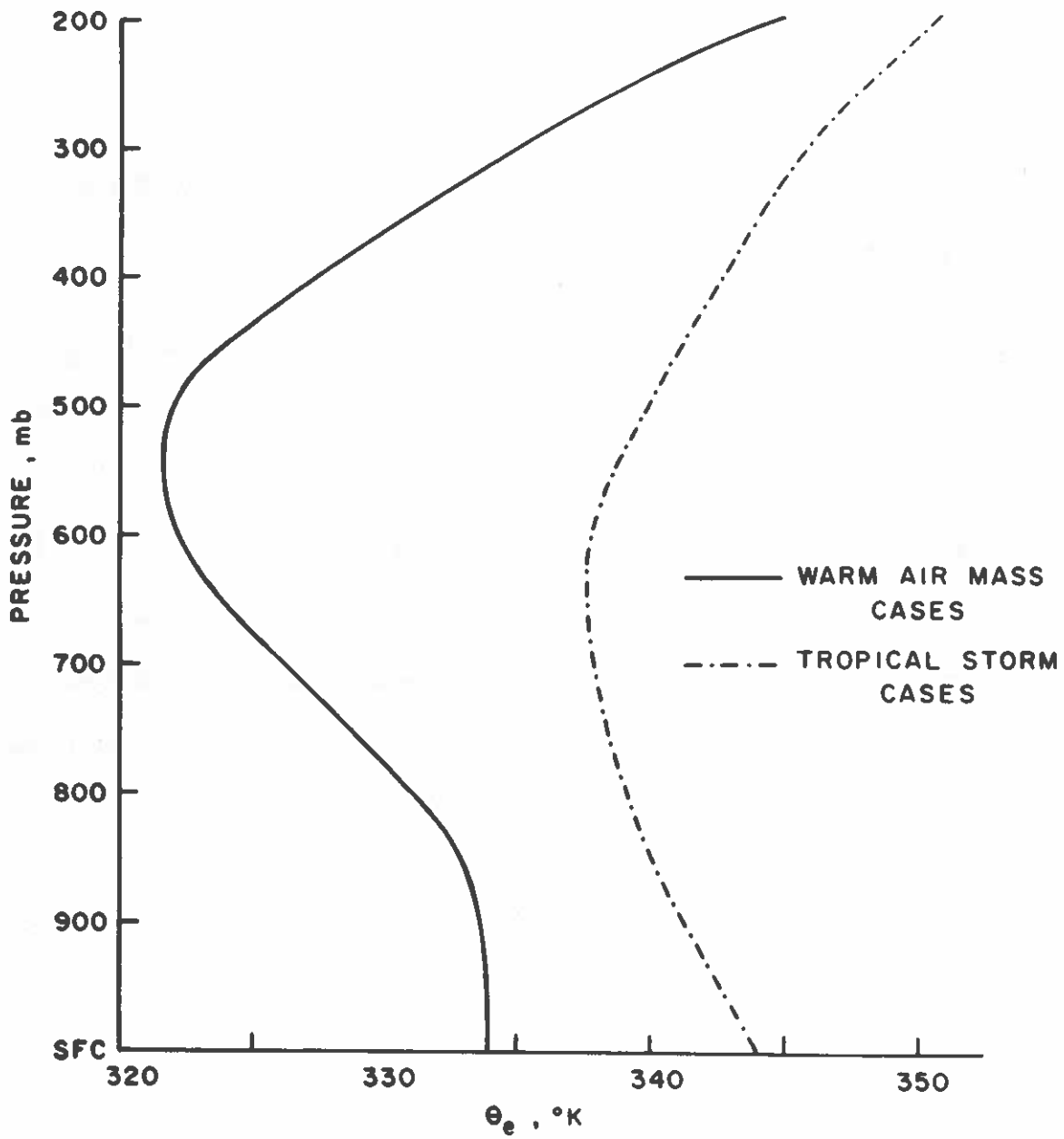

Fig. 33. Average vertical θ_e profiles for the mid-latitude warm air mass cases and the tropical storm cases.

Since thermodynamic instability indices by themselves are inadequate in explaining tropical storm spawned tornadoes, other parameters must be considered as important tornado forecasting tools. Vertical wind shear appears to be the next most important parameter. It does not appear coincidental that the major tornado producing region of the world (the eastern two-thirds of the United States) is the only area of the world where strong vertical wind shears and strong potential instability are frequently simultaneously present.

V. RELATIONSHIP BETWEEN VERTICAL SHEAR AND THE CUMULUS POTENTIAL BUOYANCY

Fig. 34 is a scatter diagram of the strongest low level shear (see discussion of Fig. 6) versus cumulus potential buoyancy for the Great Plains warm air mass cases of June through September. Post cold front cases have been eliminated. The quasi-vertical line is a 50% line for the vertical shear values--one-half the values are to the left and one-half to the right. The quasi-horizontal line is a 50% line for the cumulus potential buoyancy values. The point of intersection of these two lines establishes the median vertical shear and median cumulus potential buoyancy for this set of data.

Since the 50% lines are not perpendicular, there is evidence of a slight correlation of parameters. The correlation, however, is so small as to indicate that they are nearly independent. In this case, either parameter might be considered to be an equally good tornado predictor. Individual examination of the two parameters, however, shows that this is not the case. The cumulus potential buoyancy present in the tropics daily equals or exceeds the cumulus potential buoyancy noted for the mid-latitude tornado cases. Yet tornadoes are rare in the tropics. In the opposite sense, vertical wind shears equal to or greater than the shears shown by this study are present almost daily over the mid-latitudes during winter. Very few tornadoes are reported in the winter months, however. Thus, neither vertical wind shear nor cumulus potential buoyancy are adequate parameters by

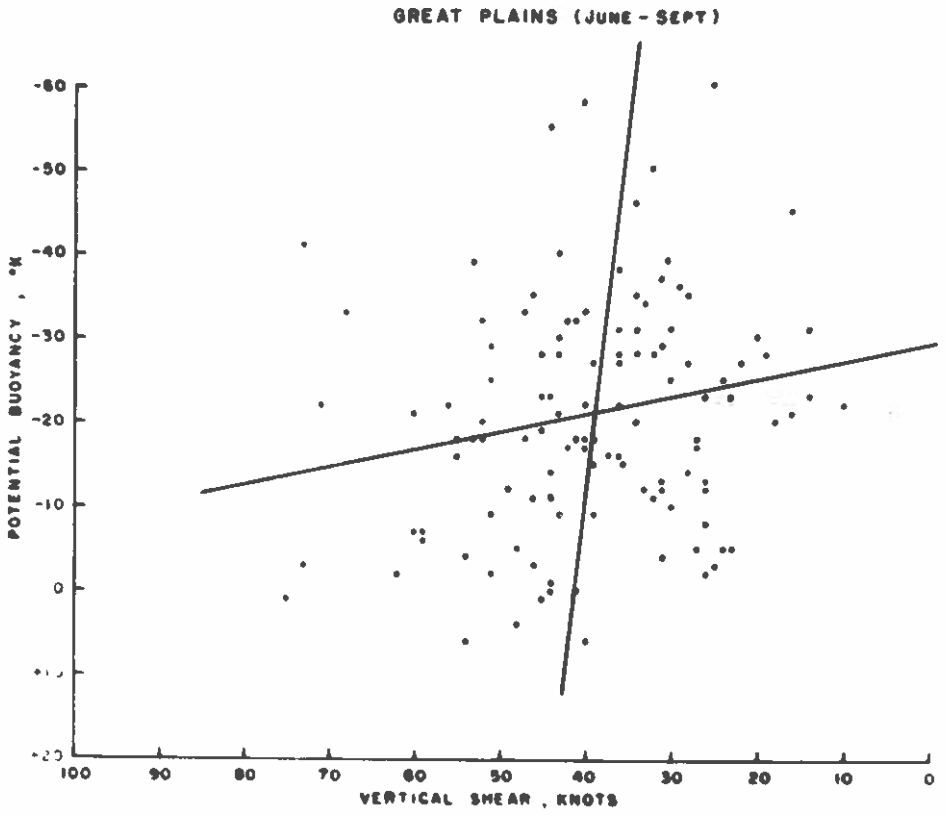

Fig. 34. Scatter diagram of Cumulus Potential Buoyancy [$\theta_{e_{min}}$ (above surface) - $\theta_{e_{sfc}}$] vs magnitude of lower tropospheric (below 500 mb) vertical vector wind shear for Great Plains cases of June through September.

themselves. When both parameters are used together, however, tornado potential can be more accurately specified.

VI. TORNADO-LIKELIHOOD INDEX

Since vertical wind shear and cumulus potential buoyancy have been described as being important for tornado occurrence, these two parameters might be combined into a tornado forecasting index. A "Tornado-Likelihood Index" (TLI) has thus been developed which also includes an estimate of the low-level convergence and, therefore, a measure of the number or density of cumulus produced by the synoptic-scale flow. The convergence parameter is essential because the vertical wind shear and potential instability by themselves do not prescribe the actual likelihood for individual cumulus development. Regardless of the instability, cumulus clouds will not occur unless sub-cloud layer convergence is present. This index has the advantage of being easy to calculate from radiosonde data or from surface and 500 mb prognosis charts.

These three parameters, the vertical wind shear (S), the cumulus potential buoyancy (CPB) and the low-level convergence (C), have been combined to form this Tornado Likelihood Index (TLI). The first term gives a measure of vertical wind structure of the atmosphere while the last two terms specify the potential intensity and density of cumulonimbus. These three parameters are unique in that they numerically measure most of the features for which tornado forecasters look (either directly or indirectly) and they have all been specified [Markgraf (op. cit.), Bates (op. cit.), and Gray (op. cit.)]

as crucial parameters in the actual tornado genesis mechanism.

For the Tornado Likelihood Index, the three parameters are specified as such:

1. S (in knots) is the largest vertical vector wind Shear between any two standard pressure levels below 500 mb.

2. CPB (in $^\circ$ K) represents a measure of the Cumulus Potential Buoyancy.

   $$CPB = -\Delta\theta_e$$

   where $\Delta\theta_e = [\theta_e$ (coldest) $- \theta_e$ (surface)]. θ_e (coldest) is the lowest θ_e observed (either 850 mb, 700 mb, or 500 mb level). If $\Delta\theta_e > 0$, CPB is negative and cumulus convection is not likely. In these latter cases, CPB is set equal to zero.

3. C (in knots) is a crude measure of the low-level Convergence. In addition to the potential buoyancy, low level convergence is necessary for cumulus or cumulonimbus production. This parameter is difficult to define from a single rawin station. For simplicity in this study, C was arbitrarily defined to be the average of the combined surface and 850 mb wind speeds. Thus, C = $\frac{1}{2}$[surface wind (in knots) + 850 mb wind (in knots)]. Physically, large values of the low level wind imply large horizontal wind shear gradients and thus large values of frictionally induced boundary layer convergence. Alternately it would have been better to have directly calculated this parameter from surface maps. The latter procedure is recommended for operational use.

The Tornado-Likelihood Index (TLI) is calculated by multiplying the magnitudes of these three parameters together and dividing by 1000, thus

$$TLI = \frac{(S)(CPB)(C)}{1000} .$$

The range of the values is from 0 to greater than 100. Seldom, however, is the TLI observed to be larger than 40.

From the previous discussion, the average tornado requirements for cumulus potential buoyancy and vertical wind shear were:

$CPB = -\Delta\theta_e \sim 15^\circ$ K,
$S \sim 45$ knots, and an average value for C is
$C \sim 25$ knots.

Thus the expected TLI value for an average tornado would be approximately

$$TLI = \frac{(45)(15)(25)}{1000} \sim 17$$

A computer program was written and used to calculate and plot the TLI for the 00Z sounding of each U.S. radiosonde station east of the Rocky Mountains for the month of May, 1965. A typical forecast output is shown by Fig. 35.

The results of the 31 days showed 19 days classified as "good." This means the TLI accurately predicted areas of severe weather and tornado outbreaks or predicted no severe weather when none occurred. Six days were classified as "fair." This classification was used when the TLI had values of approximately 13-15 in an area where tornadoes occurred, but the value did not exceed 17. A classification of "poor" was used for the six days when the TLI did not forecast tornadoes and one or more were reported or when the TLI forecast tornadoes and none occurred. Thus, for this small sample, the TLI was "good" 60% of the time and was acceptable about 80% of the days. It is doubtful that any other presently used tornado indices would have worked as well.

The greatest advantage the TLI has over the other severe weather forecasting indices is that the shear parameter selectively eliminates most of the area which thermodynamic indices rate as

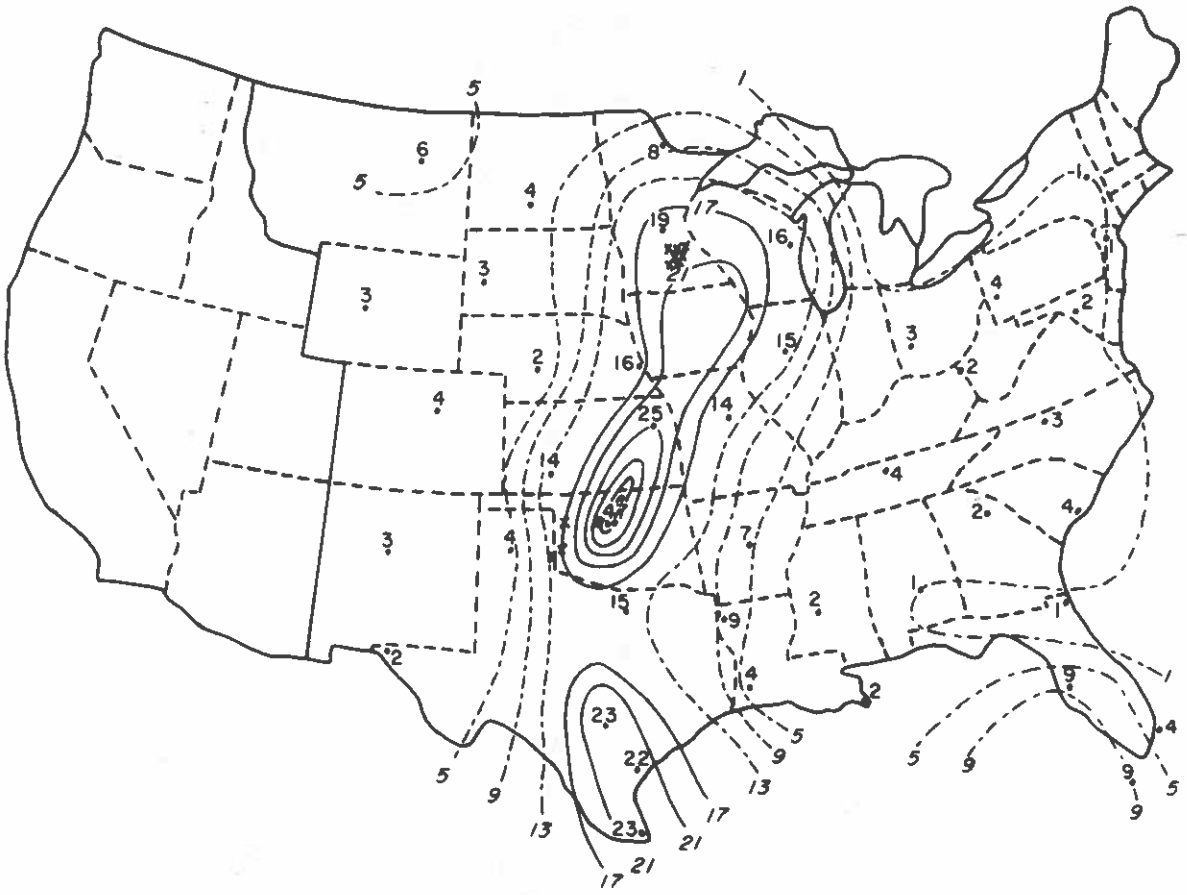

Fig. 35. Analysis of the Tornado Likelihood Index (TLI) for 00Z, 7 May 1965. Locations of tornado occurrences within two hours of 00Z are plotted with an X.

susceptible to severe weather. Thus, the TLI isolates a much smaller and, theoretically, more susceptible area for severe weather outbreaks than do purely thermodynamic indices.

As with most forecast indices [Endlich and Mancuso (op. cit.), Darkow (op. cit.)], the TLI is very accurate in predicting the "classical" severe weather outbreaks, but often falters on the marginal days when one or two isolated tornadoes are reported. These isolated tornadoes probably result from local highly favorable small scale shear and buoyancy parameter deviations from radiosonde-measured conditions.

Because of the simplicity of the TLI and its general reliability, a local observer can quickly tell from a radiosonde report or a forecast sounding whether or not his area is susceptible to a tornado. The index is also applicable to a long range severe weather outlook when combined with 24 and 48 hour numerical predictions of wind, temperature and moisture fields.

VII. SUMMARY

Most of the world's tornadoes are produced over the eastern two-thirds of the U. S. (particularly the Great Plains states) because it is only in this area that air masses possessing large potential instability are mutually present within strong vertical wind shear (baroclinic) zones.

The statistical sampling of this study has shown the vertical wind shear in the tornado environment to be positive and very large, even for tropical storm induced tornadoes. The flow patterns of the composite tornado horizontal wind field have been shown to conform in the mean to two individual case studies [Fujita and Grandoso (op. cit.) Fujita and Bradbury (op. cit.)] in which a large cumulonimbus cloud acted as a block to the mean wind field. The various flow patterns resulting from the presence of the block have been analyzed and discussed.

Thermodynamic aspects from the mean sounding data have reaffirmed previous studies. Tropical storm induced tornado potential instability, however, is shown to be of less intensity than the mid-latitude cases.

These observations support the argument that both thermodynamic and wind shear effects must simultaneously be incorporated into any tornado forecasting technique. A Tornado-Likelihood Index has been developed which includes a thermodynamic instability

parameter, a low-level convergence parameter, and a vertical wind shear parameter. This index is believed to be superior to forecasting indices based only on thermodynamic considerations. It is recommended that this type of index be further perfected for inclusion in future operational objective tornado forecasting schemes.

ACKNOWLEDGMENTS

The author wishes to express his appreciation to Professor William M. Gray who suggested this research and offered much advice and encouragement throughout its conduct. Frequent and thoughtful discussions with Mr. Charles F. Chappell during the course of this study have enabled the author to gain a greater insight into the subject. Mrs. Gladys Odle, Mr. Mamdouh Abdallah and Mr. David Ingraham are to be thanked for their help in reducing and compiling the data. The drafting of the figures by Mrs. Marilyn Setnicka and the typing of the manuscript by Mrs. Dawn Janowski are deeply appreciated.

This research has been financially supported by the National Science Foundation and by the Environmental Science Services Administration.

REFERENCES

Bates, F.C., 1967: A general theory of thunderstorms. Proceedings of the Fifth Conference on Severe Local Storms, St. Louis, Missouri.

Beebe, R.G., 1958: Tornado proximity soundings. Bull. Amer. Meteor. Soc., Vol. 39, pp. 195-201.

Bilancini, R., 1962: Ancora sulls origine delle trombe. Rivista di Meteorologia Aeronautica, Anno XXII, n. 2.

Bonner, W.D., 1963: Thunderstorms and the low-level jet. Mesometeorology Research Paper No. 22, University of Chicago, 23 pp.

Bonner, W.D., 1965: Statistical and kinematical properties of the low-level jet stream. Satellite Mesometeorology Research Project, Res. Paper 38, University of Chicago, 55 pp.

Crumrine, H.A., 1965: The use of the 850-500 mb thickness, the 850-500 mb thickness change and the 850-500 mb shear wind in severe thunderstorm forecasting, USWB Library, Kansas City, Missouri.

Darkow, G.L., 1967: The total energy environment of severe storms. Proceedings of the Fifth Conference on Severe Local Storms, St. Louis, Missouri.

Endlich, R.M. and R.L. Mancuso, 1967: Environmental conditions associated with severe thunderstorms and tornadoes. Final Report of Stanford Research Institute Project 5871.

Fawbush, E.J. and R.C. Miller, 1952: A mean sounding representative of the tornado air mass. Bull. Amer. Met. Soc., Vol. 33, No. 7, pp. 303-307.

Fawbush, E.J. and R.C. Miller, 1954: The types of air masses in which North American tornadoes form. Bull. Amer. Met. Soc., Vol. 35, pp. 154-165.

Fujita, T. and J. Arnold, 1963: Preliminary result of analysis of the cumulonimbus cloud of April 21, 1961. Satellite Mesometeorology Research Project, Res. Paper 16, University of Chicago, 16 pp.

Fujita, T. and H. Grandoso, 1968: Split of a thunderstorm into anticyclonic and cyclonic storms and their motion as determined from numerical model experiments. J. Atmos. Sci., Vol. 25, pp. 416-439.

Fujita, T. and D. Bradbury, 1969: Determination of mass outflow from a thunderstorm complex using ATS-III pictures. Paper presented at the Sixth Conference on Severe Local Storms, Chicago, Illinois, 6 pp.

Galway, J.G., 1956: The lifted index as a predictor of latent instability. Bull. Amer. Met. Soc., Vol. 36, pp. 528-529.

Goldstein, M.G., 1968: Differential advection associated with tornadoes of tropical cyclone origin. Master of Science Thesis, New York University, 33 pp.

Gray, W.M., 1967: The mutual variation of wind, shear, and baroclinicity in the cumulus convective atmosphere of the hurricane. Mon. Wea. Rev., Vol. 95, pp. 55-73.

Gray, W.M., 1969: Hypothesized importance of vertical wind shear in tornado genesis. Sixth Conference on Severe Local Storms, Chicago, Illinois.

Hill, E.L., W. Malkin, and W.A. Schultz, Jr., 1966: Tornadoes associated with cyclones of tropical origin--practical features. Jour. Appl. Met., Vol. 5, pp. 745-763.

Jordan, C.L., 1962: Vertical wind shear observations from tornado proximity soundings. Conference on Severe Storms, Norman, Oklahoma, 11 pages.

Markgraf, H., 1961: Zur Theorie der Tromben. Arch. Met. Geoph. Bioklim., S.A., B. 12, H. 3.

Miller, R.C., 1967a: Notes on analysis and severe-storm forecasting procedures of the Military Weather Warning Center. AWS TR 200.

Miller, R.C., 1967b: Semi-objective evaluation of the relative importance of parameters favoring production of severe local

storms. Proceedings of the Fifth Conference on Severe Local Storms, St. Louis, Missouri.

Miller, R.C., A. Waters, and L. Bartlett, 1965: The use of the 500/850 mb totals in severe weather forecasting. Internal Publications, USWB, Kansas City, Missouri.

Newton, C.W. and H.R. Newton, 1959: Dynamical interactions between large convective clouds and environment with vertical shear. J. Met., Vol. 16, pp. 483-496.

Newton, C.W., 1962: Dynamics of severe convective storms. NSSP Project Reports No. 9, 44 pp.

Pearson, A.D., and A.F. Sadowski, 1965: Hurricane induced tornadoes and their distribution. Mon. Wea. Rev., Vol. 93, pp. 461-464.

Showalter, A.K., 1953: A stability index for forecasting thunderstorms. Bull. Amer. Met. Soc., Vol. 34, p. 250.

Wegener, A., 1928: Beiträge zur Mechanik der Tromben und Tornadoes. Meteorol. Zeitschr., B. 45, H. 6.